



**HAL**  
open science

## **Statistical hydrology for evaluating peatland water table sensitivity to simple environmental variables and climate changes application to the mid-latitude/altitude Frasné peatland (Jura Mountains, France)**

Guillaume Bertrand, Alex Ponçot, Benjamin Pohl, Alexandre Lhosmot, Marc Steinmann, Anne Johannet, Sébastien Pinel, Huseyin Caldirak, Guillaume Artigue, Philippe P. Binet, et al.

### ► **To cite this version:**

Guillaume Bertrand, Alex Ponçot, Benjamin Pohl, Alexandre Lhosmot, Marc Steinmann, et al.. Statistical hydrology for evaluating peatland water table sensitivity to simple environmental variables and climate changes application to the mid-latitude/altitude Frasné peatland (Jura Mountains, France). *Science of the Total Environment*, 2021, 754, 141931 (55 p.). 10.1016/j.scitotenv.2020.141931 . insu-02921354

**HAL Id: insu-02921354**

**<https://insu.hal.science/insu-02921354v1>**

Submitted on 25 Aug 2020

**HAL** is a multi-disciplinary open access archive for the deposit and dissemination of scientific research documents, whether they are published or not. The documents may come from teaching and research institutions in France or abroad, or from public or private research centers.

L'archive ouverte pluridisciplinaire **HAL**, est destinée au dépôt et à la diffusion de documents scientifiques de niveau recherche, publiés ou non, émanant des établissements d'enseignement et de recherche français ou étrangers, des laboratoires publics ou privés.

## Journal Pre-proof

Statistical hydrology for evaluating peatland water table sensitivity to simple environmental variables and climate changes application to the mid-latitude/altitude Frasne peatland (Jura Mountains, France)



Guillaume Bertrand, Alex Ponçot, Benjamin Pohl, Alexandre Lhosmot, Marc Steinmann, Anne Johannet, Sébastien Pinel, Huseyin Caldirak, Guillaume Artigue, Philippe Binet, Catherine Bertrand, Louis Collin, Geneviève Magnon, Daniel Gilbert, Fatima Laggoun-Deffarge, Marie-Laure Toussaint

PII: S0048-9697(20)35460-7

DOI: <https://doi.org/10.1016/j.scitotenv.2020.141931>

Reference: STOTEN 141931

To appear in: *Science of the Total Environment*

Received date: 21 May 2020

Revised date: 30 July 2020

Accepted date: 22 August 2020

Please cite this article as: G. Bertrand, A. Ponçot, B. Pohl, et al., Statistical hydrology for evaluating peatland water table sensitivity to simple environmental variables and climate changes application to the mid-latitude/altitude Frasne peatland (Jura Mountains, France), *Science of the Total Environment* (2020), <https://doi.org/10.1016/j.scitotenv.2020.141931>

This is a PDF file of an article that has undergone enhancements after acceptance, such as the addition of a cover page and metadata, and formatting for readability, but it is not yet the definitive version of record. This version will undergo additional copyediting, typesetting and review before it is published in its final form, but we are providing this version to give early visibility of the article. Please note that, during the production process, errors may be discovered which could affect the content, and all legal disclaimers that apply to the journal pertain.



Statistical hydrology for evaluating peatland water table sensitivity to simple environmental variables and climate changes Application to the mid-latitude/altitude Frasne peatland (Jura Mountains, France)

<sup>1\*</sup>Guillaume Bertrand, <sup>1\*</sup>Alex Ponçot, <sup>2</sup>Benjamin Pohl, <sup>1</sup>Alexandre Lhosmot, <sup>1</sup>Marc Steinmann, <sup>3</sup>Anne Johannet, <sup>3</sup>Sébastien Pinel, <sup>3</sup>Huseyin Caldirak, <sup>3</sup>Guillaume Artigue, <sup>1</sup>Philippe Binet, <sup>1</sup>Catherine Bertrand, <sup>4</sup>Louis Collin, <sup>4</sup>Geneviève Magnon, <sup>1</sup>Daniel Gilbert, <sup>5</sup>Fatima Laggoun-Deffarge, <sup>1</sup>Marie-Laure Toussaint

\*These authors share the co-first authorship

<sup>1</sup>University of Bourgogne Franche-Comté, UMR UFC CNRS 6249 Chrono-Environnement, 1- route de Gray 25000 Besançon ; 4 place Tharradin 25200 Montbéliard, France guillaume.bertrand2@univ-fcomte.fr ; alex.poncot@edu.univ-fcomte.fr

<sup>2</sup>Biogéosciences, UMR6282 CNRS / University of Bourgogne Franche-Comté, 6 boulevard Gabriel, F-21000 Dijon, France

<sup>3</sup>IMT Mines Ales, 8, rue Jules Renard 30319 Alès cedex, France

<sup>4</sup>EPAGE Syndicat Mixte Haut-Doubs Haute-Loue, 3 rue de la gare - 25560 Frasne, France

<sup>5</sup>ISTO, Université d'Orléans UMR CNRS BRGM 7327, 45071, Orléans, France

**Keywords:** Peatland, Statistical modeling, Climate change, Water Table Depth, Jura Mountains, France

## Abstract

Peatlands are habitats for a range of fragile flora and fauna species. Their eco-physicochemical characteristics make them as outstanding global carbon and water storage systems. These ecosystems occupy 3% of the worldwide emerged land surface but represent

30% of the global organic soil carbon and 10% of the global fresh water volumes. In such systems, carbon speciation depends to a large extent on specific redox conditions which are mainly governed by the depth of the water table. Hence, understanding their hydrological variability, that conditions both their ecological and biogeochemical functions, is crucial for their management, especially when anticipating their future evolution under climate change. This study illustrates how long-term monitoring of basic hydro-meteorological parameters combined with statistical modeling can be used as a tool to evaluate i) the horizontal (type of peat), ii) vertical (acrotelm/catotelm continuum) and iii) future hydrological variability. Using cross-correlations between meteorological data (precipitation, potential evapotranspiration) and water table depth (WTD), we primarily highlight the spatial heterogeneity of hydrological reactivity across the *Sphagnum*-dominated Frasne peatland (French Jura Mountain). Then, a multiple linear regression model allows performing hydrological projections until 2100, according to regionalized IPCC RCP4.5 and 8.5 scenarios. Although WTD remains stable during the first half of 21<sup>st</sup> century, seasonal trends beyond 2050 show lower WTD in winter and markedly greater WTD in summer. In particular, after 2050, more frequent droughts in summer and autumn should occur, increasing WTD. These projections are completed with risk evaluations for peatland droughts until 2100 that appear to be increasing especially for transition seasons, i.e. May-June and September-October. Comparing these trends with previous evaluations of phenol concentrations in water throughout the vegetative period, considered as a proxy of plant functioning intensity, highlights that these hydrological modifications during transitional seasons could be a great ecological perturbation, especially by affecting *Sphagnum* metabolism.

## 1. Introduction

Fresh water resources have become a global challenge from a sociological and ecological point of view. The global demographic evolution makes it difficult to supply the increasing demand and amplifies social disparities between and within countries (Piao et al., 2010). Socio-environmental tensions are expected to increase warming and possible alterations in precipitation regimes (e.g., Vorosmarty, 2000; Kløve et al., 2014). Climate change is projected to lead to increasing extreme meteorological events (droughts, floods), impacting even temperate areas such as Western Europe, (Brulebois et al., 2015a). It is thus expected to create major water resource issues. Therefore, in order to adapt current practices and to preserve the resource, managers require a detailed evaluation of the further evolution of water availability for socio-ecosystems. In parallel, due to the current stakes in limiting global carbon emissions and sustaining biodiversity (Paris Agreement, 2015; Bongaarts, 2019), an integrated overview of the possible evolutions of hydrological, biogeochemical and ecological functions of socio-ecosystems is necessary.

In this context, peatlands, representing 3% of the worldwide emerged land surface, are hotspots of major socio-environmental interests as they represent 10 % of the global freshwater volumes and 30 % of the organic carbon contained in soil (Joosten, 2016). Peatlands are usually found in regions with humid climate and favorable local geomorphological features (Lavoie et al., 1995). These contexts promote anaerobic conditions, limiting mineralization of organic carbon and related gaseous carbon emissions of from ecosystem respiration. Over the long-term, ecosystem respiration is balanced by gross primary production through photosynthesis, which eventually induces a net atmospheric carbon capture (e.g., Augustin et al., 1998; Kang et Freeman, 2002). In addition, plant species restricted to peatlands, such as bryophytes like the *Sphagnum* genus, modify their immediate chemical environment through the release of organic acids. This favors oligotrophic anoxic conditions, slowing down the microbially induced mineralization of organic matter (e.g.,

(Preston et al., 2012). This is amplified by the production of polyphenolic compounds, which are known to have a strong inhibitory effect on microbial breakdown of organic matter (Verhoeven and Toth, 1995; Jasse et al., 2011). Peatland ecosystems are therefore significant carbon stocks, whose stabilization is promoted by saturation in water, either coming directly from precipitation or from surface runoff and groundwater (Bertrand et al., 2012 and references therein). Hence, It is currently discussed whether peatlands may, together with other wetlands, act as buffer reservoirs for carbon and water and smooth the flow regime in the downstream parts of their watershed (Martin and Didon-Lescot, 2007; Xu et al., 2018).

The current warming and associated modification of precipitation regimes (Trenberth, 2011), altering hydrological conditions ensuring water supply of these systems, may consequently affect specific physico-chemical and ecological conditions favoring carbon storage and thus in turn amplify climate change (Laggoun-Défarge et al., 2016). Moreover, because bryophytes are non vascular plants, a recurring drawdown of water levels could affect their physiological activities and finally favor their replacement by non-peat forming vegetation, e.g., shrubs (Buttler et al., 2015).

Therefore, the understanding of the water table reactivity of peatlands to climate changes is a prerequisite to evaluate their further impact on water resources and carbon fluxes. The study of the hydrological reactivity of a wetland ideally requires a clear delineation of the catchment and a description of its hydraulic characteristics. Nevertheless, these evaluations are in most cases difficult to obtain at the watershed and ecosystem scales. At the watershed scale, this characterization may be expensive and time consuming. Furthermore, it is challenging to upscale local observations to catchment scale, especially in areas with complex geomorphology. At the ecosystem scale, the strong hydraulic heterogeneity of the organic matrix, which undergoes humification at variable time rates due to heterogeneous environmental conditions, is a challenging issue (Wastiaux, 2008). The lack

of detailed spatial data and associated parameterization implies that the hydrological response cannot be easily modeled by simple physically-based approaches (Okkonen and Kløve, 2010). A similar heterogeneity is for example known for karst systems, with very dissimilar transfer velocities in open conduits vs. micro-fractured rock (Delbart et al., 2014 and references therein).

In order to overcome such heterogeneity-related issues, modeling approaches based on correlation analyses were developed principally by Jenkins and Watts (1968) and Box et al. (1994), and adapted to karstic systems by Mangin (1975). In these approaches, the hydrological system is considered as a filter transforming an input signal (*e.g.* P, T, evapotranspiration) into an output signal (discharge, water level) by a transfer function (Mangin, 1984). Once defined, this function can be interpreted to assess the functioning, organization and structure of the hydro-ecosystem and subsequently, the response can be used to build a regression model of the hydrological response (Chen et al., 2002). Thus, supposing, in first approximation, that the behavior could be considered, at a given time-step, as linear and time-invariant, statistical methods in general can be used as a primary assessment tool where physically-based models would be difficult to implement. Various studies have demonstrated the ability of such regressive models to predict changes in water table variations (Bierkens et al., 2001; Okkonen and Kløve, 2010; Viswanathan, 1983). They are therefore an appropriate approach to model the present and future hydrological behavior of complex hydroecosystems such as peatlands (Okkonen and Kløve, 2010).

In this perspective, this work aims at illustrating how hydrometeorological monitoring over peatlands and the use of cross-correlations and multiple linear regression methods can be used by environmental managers in order to evaluate the spatio-temporal heterogeneity of WTD fluctuations and model the future WTD response to climate changes.



## 2. Context of the study

### a. Localization of the Frasne peatland

The study site is a *Sphagnum* peatland located near Frasne in the French Jura Mountains (46.826 °N, 6.1725 °E : z= 852 m.asl, Figure 1). It occupies 7 ha of a vast depression located in the upstream part of the Dugeon catchment and belongs to a larger peatland complex of 300 ha of varying evolution stages (Gauthier et al., 2019). The site is part of the Regional Natural Reserve (RNR) of Frasne-Bouverans composed of remarkable wetlands included in the Ramsar international agreement (1971), the Natura 2000 network (European "habitat" and "birds" directives) and constituted of various Natural Zones of Floristic and Faunistic Ecological Interest (ZNIEFF) of type 1 and 2. The study site is also called “the active peatland”, as terrestrialization is currently ongoing.

### b. Geological and pedological context

From a geological point of view the Jura Mountains features a succession of SW-NE trending anticlines and synclines affecting mainly limestones and marls of the Jurassic and Lower Cretaceous. Subsequent erosion shaped the topography and favored the formation of karstic landforms (Figure 2). In synclines this geomorphology is partially overlain by impervious or semi-impervious Quaternary moraines, favoring the occurrence of lakes and wetlands (e.g. Saint-Point, Joux lakes). Consistently, the Frasne peatland is located in an open syncline covered by heterogeneous moraines promoting water retention. This favored terrestrialization and the gradual closure of open water expanses.

The pedological description of the active peatland was carried out by Briot (2004). The soil profiles are over 2 m deep, consisting of blond peat in the central area (Figure 1). The fiber content is high at the surface, with high apparent hydraulic conductivities (K) and pH values ranging between 5.5 and 8.5 (Briot, 2004). In contrast, the adjacent wooded peatland is

dominated by brown peat with thicknesses up to 5 m (Gauthier et al., 2019). The transition between these two main peat types is gradual, with less fibric peat in the peripheral zone of the active peatland (Figure 1).

### c. Hydrological framework

The climate of the site is mountainous with oceanic influence, characterized by almost constant monthly rainfall throughout the year in the range of 80 to 120 mm / month. In contrast, the monthly mean temperatures are very variable, ranging between 0 and 15° C in February and July, respectively, for an annual average of 6.5° C (1981-2010: Meteo-France, 2019). This value was, according to our local site observatory platform, 6.9 °C for the monitoring period (2009-2019) (Toussaint et al., 2023a).

The particular geological and geomorphological context implies a complex hydro(geo)logical functioning of the system. Although water supply is at least partly ensured by direct rainwater infiltration, concurrent inflows from surrounding surface areas or from underlying moraines fed by deeper karstic systems have also been suggested on the basis of geochemical indices (Collin, 2015; Lhosmot et al., 2019). In addition, local or regional geomorphological evidence, such as karstic springs, dolines and sinkholes, suggests the possibility of local hydraulic connections with the regional karst aquifer. This is in particular the case for a sinkhole located south of the study site named "*Creux au lard*" ("the bacon dip"), which drains today a part of the peatland outflow and which is, according to dye tracer tests, connected with the karst spring of the Ain river, located 14 km to the SW (Figure 1; Briot, 2004). However, coring investigations have shown, in agreement with geomorphological observations, that the "*Creux au lard*" was in the past probably an inversac structure rather than a simple sinkhole, acting either as a sink or as a source, depending on weather conditions and season (Thomas, 2015). Other karstic vents are likely present under the peaty layer which could potentially influence the water balance of the system (Collin,

2016). In addition, the Frasne peatland was impacted by human activities since the 19<sup>th</sup> century by the installation of drainage ditches south and east of the living peatbog, which affected the hydrology of the site (Grosvernier, 2014; Collin, 2016). Most of these ditches were backfilled in a restoration program implemented in 2015 in the framework of the European Life Jura Peatland program (Calvar et al., 2018).

This overall context illustrates the geological, geomorphological, and the structural complexity of the Frasne peatland, making it difficult to constrain mechanistically the processes and parameters controlling water supply, storage, and transfer to downstream hydrosystems, thus justifying the use of a modeling approach based on correlation analyses rather than on mechanistic concepts.

#### **d. Projected climatic evolutions**

The Intergovernmental Panel on Climate Change (IPCC, 2014) proposed four main Representative Concentration Pathways (RCPs) scenarios that integrate possible future greenhouse gas emission trajectories to force climate models and thereby provide climate change projections until 2100. RCPs are named after the additional radiative forcing calculated between 2100 and the pre-industrial era, and resulting mostly from the combustion of fossil fuels. For instance, RCP2.6 corresponds to an additional forcing (and thus additional greenhouse effect) of  $+2.6 \text{ W. m}^{-2}$  and represents the case of early and major political mitigation efforts. In contrast, RCP8.5 proposes weak political effort to reduce greenhouse gas emissions and reaches  $+8.5 \text{ W.m}^{-2}$  in the late century. Two intermediate scenarios were also proposed, namely RCP4.5 and RCP6.0.

For impact studies and analysis of climate change at fine scales, regional downscaling of global climate simulations is provided by the Euro-CORDEX modeling exercise (Jacob et al., 2014). Over the territory of Metropolitan France, Euro-CORDEX simulations were regridded

at a 8x8 km horizontal resolution and bias-corrected against reference SAFRAN reanalysis (Vidal et al., 2010) using the CDF-t methodology developed by Michelangeli et al. (2009). This method adjusts the statistical distribution function of a simulated variable to reference climate observations under present-day conditions, and applies the same transformation for future periods. The resulting dataset is appropriate for impact studies of climate change and is available for RCP4.5 and RCP8.5 for 7 regional models and for the period 2006-2100. The use of an ensemble of climate models allows for a quantification of model-dependency and associated uncertainties. It also makes it possible to disentangle climate responses to external forcings and natural climate variability.

According to this downscaled database for the Frasne area (Figure 3), mean temperature should increase in any case throughout the year. Both RCP4.5 and 8.5 scenarios imply a similar thermic regime for the 2040-2070 period (respectively  $8.8 \pm 0.4$  °C and  $9.5 \pm 0.4$  °C). RCP4.5 leads to a stabilization of this new state of the climate by 2070-2100. In contrast, the RCP8.5 should induce a further warming ( $10.6 \pm 0.6$  °C), corresponding to an increase of 3.7° C against the 2005-2019 observational period, and 4.0 degrees against the reference period (1980-2010). Regarding precipitation trends, both RCPs result in an increase for spring (March, April, May, June) of about  $+0.5 \text{ mm.day}^{-1}$ , a strong decrease in July and August (from  $-1 \text{ mm/d}$  for 2040-2070 to  $-1.5 \text{ mm.day}^{-1}$  from 2070/2100 for the RCP8.5). In autumn, October should feature the largest changes (between  $+1.2$  and  $+1.5 \text{ mm.day}^{-1}$ ). November and December should present similar amounts for any RCP at both 2040-2070 and 2070-2100 horizons. The study site is thus representative of large parts of Western Europe, where changes in precipitation concern more their distribution within the annual cycle than their overall amounts (IPCC, 2014).

### 3. Materials and methods

The aforementioned geological, geomorphological and future climate contexts imply a high degree of complexity that makes difficult the adaptation of the management of the Frasne peatland.

In the approach proposed for this work, precipitation (P) corresponds to the primary input signal at the watershed and ecosystem scale. Along with downward percolation, rainwater interacts with solid materials (e.g. adsorption) and reconstitutes the Easily Usable water Reserve (EUR, Gendry 2018). It is the water volume available for vegetation, its availability depends on one hand on the nature of soil (i.e. abundance and quality of clay minerals and organic matter), and on the other hand on meteorological variables (P, T, wind, solar radiation). These variables impact evapotranspiration (ET), whose variability can be estimated through an evaluation of the potential evapotranspiration (PET: Bouchet 1963).

The difference between P minus ET and  $\Delta EUR$  (change of EUR between two dates) is called effective rain (ER), which corresponds to the fraction of precipitation available for infiltration (Eq.1).

$$ER = P - ET - \Delta EUR \quad (\text{Eq. 1})$$

Assessing the spatio-temporal variability of all these variables would require a large range of analyses, and the implementation of the resulting data set into a comprehensive model would be demanding and time-consuming. Therefore, we propose a simpler and potentially more robust model based only on estimators directly derived from meteorological variables monitored over the peatland and an estimation of PET.

#### **a. Hydrometeorological data**

Since 2012, the National Observatory of Peatlands (“SNO Tourbières”, led by the French national research institute CNRS) is in charge of the environmental monitoring of the site, in continuity to a previous monitoring program implemented since 2008 (Jassey et al., 2011).

This monitoring includes thirty environmental, physicochemical and biodiversity variables at the ecosystem scale.

Within the framework of this study, the input data are temperature and precipitation monitored at a 30-minute time-step by a weather station located near the center of the active peatland (Figure 1, Toussaint et al., 2020a;b). Temperature is measured with a Vaisala - HMP155A probe with a precision of 0.2 °C. Precipitation data are acquired by a CEH – ARG100 pluviometer with a precision of 0.2 mm. Potential evapotranspiration variability is computed using the equation of Oudin et al. (2005). This method requires only temperature as input variable. PET is then calculated according to the Earth position and obliquity that are dependent on the Julian day for which the calculation is performed (Eq. 2).

$$PET = \frac{\frac{R_e * T + K_2}{\lambda \rho}}{K_1} \quad (\text{Eq. 2})$$

Where PET is the potential evapotranspiration (in mm. day<sup>-1</sup>), Re is the External radiation (in J.m<sup>-2</sup>.day<sup>-1</sup>) depending on the latitude and Julian day, λ is the latent heat flow (=2.45.10<sup>9</sup> J.kg<sup>-1</sup>), ρ is the water density (in kg.m<sup>-3</sup>), T is the daily air temperature (°C), K<sub>1</sub> and K<sub>2</sub> are adjustment constants.

The output data corresponding to Water Table Depth (WTD) was monitored in 14 piezometers. Ten of them (tv1 to tv6 and tv11 to tv14) are equipped with automatic HOBO pressure probes functioning at an hourly time step. For this study, we used the WTD between July 2014 and July 2018. Two other piezometers (SOwet and SOdry) equipped with automatic transducer PDCR1830 (Campbell scientific) measure WTD every 30 minutes (Figure 1). For this study we used data for the period July 2009-July 2019. In order to homogenize the dataset, and to facilitate statistical treatment, all data sets were reduced to daily time steps (daily average for temperature and WTD and daily amounts for precipitation (see *e.g.*, Figure S1).

**b. Evaluation of the hydrological response variability to meteorological inputs:  
cross-correlation, response and memory times**

Like in other hydroecosystems, WTD depends on precipitation and evapotranspiration during the preceding days (Chen et al., 2002; Okkonen and Klove, 2010). Similarly, for a given vegetation type, the capacity of a peatland to store water (“sponge effect”) tightly depends on the meteorological conditions that preceded the rain event (Wastiaux, 2008). On this basis, a linear statistical “black box” model can be implemented as a function of climatic variables (Mangin, 1984). The peatland is then assimilated to a “black box” type system whose climatic variables and water level represent respectively the inputs and the output. Analysis of the output signal can be interpreted in terms of physical properties of the system. Correlation analyses provide information on trends, periodic phenomena and storage capacities of the system.

Considering the signals as a time series, the correlation coefficient between two variables  $x$  and  $y$ , at the discrete time lag  $k$ ;  $r_k$  is defined according to the formula proposed by Jenkins and Watts (1968):

$$r_k = \frac{C_k}{C_0} \quad \text{with} \quad C_k = \frac{1}{n} \sum_{i=1}^{n-k} (x_i - \bar{x})(y_{i+k} - \bar{y}) \quad \text{and} \quad C_0 = \sigma_x \sigma_y \quad (\text{Eq 3})$$

where  $n$ : number of samples of the time series.

$k$ : temporal lag (number of time-step), with  $k = 0, 1, 2 \dots m$ .

$x_i$ : sample  $i$  of the variable  $x$ , and  $y_i$  sample  $i$  of the variable  $y$ .

$\bar{x}$ : mean of the variable  $x$ . and  $\bar{y}$ : mean of the variable  $y$ .

$m$  is the maximum value of the lag  $k$ , it is usually chosen as  $m \leq n/3$  (Mangin, 1984)

Plotting  $r_k$  versus  $k$  provides the correlogram depicting the dynamics of the system.

If  $y=x$ , the correlogram is called an auto-correlogram. The auto-correlogram allows identification of the *memory effect* (or inertia) of a system, which can be related to its storage capacity (Mangin, 1975). The memory effect is the time delay necessary to reach minimal autocorrelation, allowing to consider that the latter is negligible. For this study, memory is defined by the lag-time the auto-correlogram takes to keep a significant autocorrelation at the 95 % confidence level. If  $x \neq y$ , then the correlogram is called cross-correlogram; the cross-correlogram allows quantifying the influence of a specific input variable (*e.g.*, inputs P, T) on the output variable (*e.g.*, WTD). It is thus possible to identify the *response time* of the system, denoted as  $t_r$ , corresponding to the  $k$ -value at highest  $k$ , and the *memory time*  $t_m$ , corresponding to the delay necessary to wipe out the effect of the external influence.

Given that a restoration program consisting in backfilling of a drainage ditch close to TV14 took place in Summer 2015, which also modified the mean WTD of piezometers TV11, 12, 13, and 14 (Collin, 2016), the cross-correlation was performed only on data from September 2015 to September 2018, corresponding to four complete and undisturbed hydrological years. In contrast, the piezometers SOWet and SODry from the central area of active peatland were not affected by the restoration program (Collin, 2016), therefore the complete data set was used for these piezometers (July 2009-June 2019).

### c. Statistical modeling of water table depths

Various authors (*e.g.*, Chen et al., 2002; Okkonen and Klove., 2010) proposed that water heights (or the related WTD) may be reconstructed through to the combination of a constant (C), combined with precipitation and temperature data of the previous days, the latter being used by Chen et al. (2002) as a proxy for evapotranspiration (Eq. 4).

$$WTD(x, t, \Delta t) = C + \alpha_1 \cdot P_{lt}(t - \Delta t) + \alpha_2 \cdot P_s(t - \Delta t) + \alpha_3 \cdot P_{st}(t - \Delta t) + \beta T(t - \Delta t) \quad (\text{Eq. 4})$$



Where  $H$  : water height (in m);  $P_{lt}$ ,  $P_s$ ,  $P_{st}$  : long-term, seasonal and short term precipitation in mm;  $T$  : Temperature (in °C) ;  $C$  : a constant ;  $\alpha$  (1;2;3) and  $\beta$  : coefficient multiplying each variable.

According to Okkonen and Klove (2010), this general model needs to be calibrated for each hydroecosystem. In the case of the Frasne active peatland, various statistical models based on Chen et al. (2002) were tested including different sets of variables, in particular by directly using the mean daily  $T$  (not shown). Nevertheless, best estimates for WTD were obtained by using as input variables daily  $P$  and  $PET$  as calculated in Oudin et al. (2005). This  $PET$  estimation method integrates both  $T$  and Earth obliquity according to the Julian day that is latitude dependent. This method appears more realistic to estimate the  $T$  effect over vegetation processes affecting WTD.

Due to the absence of clear long-term and short-term trends for precipitation over the monitored period (Figure S1 in supplementary material), the delineation of  $P_{sh}$ ,  $P_s$  and  $P_{lt}$  was not successful. The absence of such trends is common for Western Europe (see Brulebois et al., 2015a), although some changes seem to have occurred recently in the 2010s. Therefore, our model uses daily precipitation data and  $PET$  values estimated by Eq. 2 rather than  $P_{sh}$ ,  $P_s$  and  $P_{lt}$  values. The memory times determined by cross correlations between  $P$ ,  $PET$  and WTD were used to evaluate the time sequence to be included in the model (Eq. 3). To ensure the linearity of the regression model and to limit possible threshold effects, the data were first log transformed (Eq. 5).

$$\left| \begin{array}{l} \log_{10}(WTD)_{S_t} = C + \sum_{i=1}^{t_i=t_{mP}} \alpha_i \cdot P_i - \sum_{j=1}^{t_j=t_{mPET}} \beta_j \cdot PET_j \\ \text{(Eq.5)} \end{array} \right.$$

| With  $(WTD)_{S_t}$  the simulated WTD for time  $t$

$P_i$  : Precipitation (in mm) of days that are comprised in the period for which  $r_k$  between WTD and P is significant i.e. between  $t_i = 1$  and  $t_i = t_{mP}$ ,  $t_{mP}$  being the memory time in days of WTD in relation to daily P;

$PET_j$  : Potential Evapotranspiration (in mm) of days that are comprised in the period for which  $r_k$  between WTD and PET is significant, i.e. between  $t_j = 1$  and  $t_j = t_{mPET}$ ,  $t_{mPET}$  being the memory time in days of WTD in relation to daily PET;

C: a constant,  $\alpha$ ,  $\beta$ : multiplying coefficients.

Model calibration was performed by determining the coefficients  $\alpha$ ,  $\beta$ , C using P and PET data covering 9 years between July 2009 and June 2018 (3285 days) from the SOwet and SOdry piezometers (Figure 1). Then, the data from July 2018 to June 2019 were used for validation. For this paper, only the results from piezometer SOdry are shown, because of its longest record (July 2009-June 2019). Calibration and validation were evaluated through to the square of the Pearson coefficient  $r^2$  (Eq. 6) and Nash-Sutcliffe Efficiency (NSE; Eq. 7). The NSE ranges from  $-\infty$  to 1. A NSE of 1 corresponds to an optimal fit, whereas NSE lower than 0 indicates that the observed mean is a better predictor than the model (Nash and Sutcliffe, 1970).

$$r^2 = \left( \frac{Cov(WTD_t, WTD_{St})}{\sigma(WTD_t)\sigma(WTD_{St})} \right)^2 \quad (\text{Eq. 6})$$

Cov is the covariance function, and  $\sigma$  the standard deviation of the considered series;

$$NSE = 1 - \frac{\sum_{t=1}^n (WTD_{St} - WTD_t)^2}{\sum_{t=1}^n (WTD_t - \overline{WTD})^2} \quad (\text{Eq. 7})$$

$WTD_{St}$  and  $WTD_t$  are the simulated WTD and the observed WTD at time t respectively,  $\overline{WTD}$  the mean observed WTD.

### Future climate change and projection of future water table depths

Seven regional climate models participating to the Euro-CORDEX exercise with post-corrected data are available in the Drias databases (Table 1). They were used to force the regressive model with the required input variables (namely daily precipitation and temperature) over the future decades. The downscaled and post-corrected projections were then compared to the monitored period (2009-2019). The effects of climate change were assessed through several statistical methods. Firstly, statistical tests linked with multiple linear model (MLR) were performed to verify the assumptions of MLR : i) The normality was tested by the Shapiro-Wilk test and the homoscedasticity by the Bartlett test; ii) the absence of multicollinearity between predictors was verified by using the pearson correlation test). Secondly, in order to statistically assess the differences between the modelled values under each RCP scenario, we used when ANOVA-1 factor, when the assumption were verified and alternatively the non-parametric Kruskal-Wallis test. All results were considered at the 95% confidence level. The homoscedasticity of the error between observed and simulated data was assessed through the Breusch-Pagan test.

As it is based on a statistical method, the proposed approach does not directly account for the possible future local vegetation changes, such as peat growth, possible colonization by vascular plants. However, the study site corresponds of a small depression of 7 ha area being part of larger peatland complex of 300 ha with an overall mature vegetation cover (pine forest over a raised peatland; Gauthier et al., 2019). Therefore, although transitions from peat to vascular vegetation may impact locally PET dynamics, we consider that the overall distribution of vegetation will not be fundamentally modified, suggesting that the future evolution of PET will mainly depend on temperature rather than on vegetation changes.

Concerning snow events, the automatic pluviometer of the monitoring platform is not equipped with a heating coil for snowfall measurements. Therefore, precipitation from snowfall may be delayed, meaning that the pluviometer actually recorded snowmelt rather

than snowfall. For the future modeling task, as the evaluation of number of snow days were evaluated on the basis of both simulated P ( $>0$ ) and T ( $<0$ ), it appears that the occurrence of snow events should, as it is the case since 2018, drastically decrease, as it is projected in mid-latitude/altitude areas (IPCC, 2014). This evaluation is shown in supplementary material (Figure S2) and supports our approach considering that low T mainly limits evapotranspiration, without having a strong impact on the general peatland behavior, in contrast to high latitude systems (e.g., Okkonen and Klove, 2010).

## 4. Results and Discussion

### a. Spatial variability of hydrological reactivity and horizontal hydraulic heterogeneity

Our WTD data show rapid responses to precipitation (Figure 4A), with response times of 1 (SOdry et SOwet) to 2 days (TV11, TV12, TV13). Only TV14 shows no significant response. The central piezometers SOdry and SOwet are more directly linked to precipitation with maximum  $r_k$ -values between P and WTD close to 0.5, whereas the relationship is weaker for the peripheral piezometers. Regarding memory times after precipitation events, the central piezometers have memory times of about 50 days, whereas the durations are shorter for the peripheral zone (22, 27 and 29 days).

In addition to these trends, except for TV14, one observes a bi-modal or tri-modal response : after the rapid response with highest  $r_k$  (1 to 2 days), more lagged and strongly buffered responses of 15 to 25 days are detected. This behavior suggests the existence of distinct water pathways from the atmosphere to the peatland and recalls the model of Ingram (1978), who distinguished three types of flows in the acrotelm: 1) fast supersaturation flows; 2) fast under-saturation flows; and 3) slow flows at the basis of the acrotelm.

Correlations between PET and WTD show a greater spatial heterogeneity, with response times varying from 35 to 82 days and memory times from 120 to 150 days (Fig. 4). The highest  $r_k$  values of 0.5- 0.6 occur for the central piezometers (SODry and SOWet) with shortest response times of 35 days, whereas the peripheral piezometers present weaker correlations ( $<0.3$ ) and longer response times (5282 days, Figure 4B). Memory times are similar for all piezometers (about 120 days), except for TV12 (about 150 days).

These results argue for a response typology according to the locations in the peatland. The faster and greater reactivity of the central piezometers (SOWet and SODry) suggests a stronger sensitivity to atmospheric and surface processes, probably due to their position within a zone with high vertical hydraulic conductivity ( $K$ ). The memory time contrast for WTD/P indicates as well that in the central area the meteoric inputs are better conserved after the faster response component while PET variability directly affect WTD (without any lag) in this area. This could be interpreted as a characteristic of an efficient lateral transfer of the most superficial processes (infiltration, evapotranspiration). In contrast, TV11, TV12 with longer response and shorter memory times after P events argue for a system with a stronger filtering capacity, likely related to a supply by a more inertial reservoir, less reactive to vertical infiltration and superficial evapotranspiration. The intermediate reactive behavior of TV13 could consequently be related to a peat matrix of intermediate vertical hydraulic conductivity. TV14 may be considered as no reactive through this approach, highlighting the great inertia of its surrounding area. This is interpreted as the effect of the restoration of the ditch located next to this piezometer (Collin, 2016) and highlights the importance of very local conditions in understanding relationships between meteorological processes and WTD.

If the difference in memory times may be the consequence of a range of factors mainly difference in horizontal  $K$  and/or local mean hydraulic gradients favoring of limiting horizontal transfers, the differences in response time may reveal  $K$  contrasts. They could be related to differences in the biogeochemical regime between the peripheral and central peatland systems, which potentially influence the compaction of the peat matrix. Mitchell et al. (2008) found that peripheral areas of raised bogs can exhibit qualitatively different biogeochemical regimes from the central part of the bog, due to the chemical composition of runoff from surrounding mineral uplands. Other studies suggest that contrasts in peat properties, structures and degradation process rates, play a key role in promoting faster peat growth rate and peat accumulation over the central part of peatlands (Lapen et al., 2005; Baird et al., 2008; Eppinga et al., 2009; Morris et al., 2011). Because of such variations, the local  $K$  is expected to be lower for the peripheral portions of blankets (Lapen et al., 2005) and raised bogs (Baird et al., 2008). In the context of the Frasne peatland, the most reactive area (SO<sub>wet</sub>/SO<sub>dry</sub>) along the vertical axis is located in the central depression zone, corresponding to the less mature, and therefore less compacted part of the peatland. In contrast, southern piezometers are located close to the edge of the active peatland site (Figure 1). Such a horizontal contrast is also consistent with peat characterizations achieved by Briot (2004). This author delineated a central part of the peatland featuring a blond fibric peat made of 70 % of fibers. In contrast, the peatland edges are characterized by a brown peat, less fibric, suggesting a longer maturation/humification (Figure 1C). Fiber content and hydraulic conductivity were shown to be linked by e.g., Boelter (1969). In addition, peat drilling until 200 cm and dating suggest that central areas feature a 930-year old peat, whereas external parts of the living peatland, at the same depth, date back from 3555 years BP (Goubet, 2015; Gauthier et al., 2019). In this peripheral area, very low  $K$  about  $10^{-8} \text{ m.s}^{-1}$  were estimated, through laboratory experiments, at 125-165 cm depth (Thomas, 2015). No values for the

central area are available so far to finalize the comparison, but our results suggesting a lower inertia for the central area would be consistent with greater K, still to be investigated.

Some additional processes and effect could be explanatory for the observed trends. The existence of an underlying karstic hydrogeological system emitting groundwater through glacial deposits (Collin, 2016) could also buffer the WTD response to rain events, through an additional –and delayed– source of water in the southern area. Although no definitive clue of such a contribution has been identified, some geomorphological and geochemical indices are in favor of this process. The observation of greater water mineralization near the base of the living peatland suggests that lateral and/or upward fluxes of mineralized water may occur (Lhosmot et al., 2019). Locally, this karstic influence could also have promoted clogging of the peat by fine mineral particles as it was suggested by punctual drilling observations (Bichet, 2014). Consistently, (Bourgault et al., 2019) highlighted that meteorological conditions have variable effects on WTD and their fluctuations in peatlands, depending on their hydrogeological settings. When an aquifer provides water to a peatland, groundwater fluxes favor the stability of WTD that appears to less react to daily meteorological processes (Kløve et al., 2014), a buffering process that depends on the aquifer type and scale (local, intermediate, regional; Perland et al., 2012). Moreover, management options such as peat material importation (next to TV14), could promote more diffuse water transfer and alter the water supply dynamics from either meteoric or subterraneous origins, amplifying contrasts between the peripheral and the central areas of the ecosystem.

Despite these potential geological and restoration effects, the cross-correlation approach based on long-term monitoring data underlines its usefulness to identify contrasts in hydrological behaviors. Although not providing a direct physical characterization, this spatial heterogeneity implies ecological contrasts that are relevant for long-term ecosystem functioning and management. The buffer capacity of the peripheral portions of the peatland,

due to their likely lower K, could smooth meteorological variability over the area (Morris et al., 2011; Mitchell et al., 2008) and maintain wet conditions in the central areas, allowing for more efficient peat development (Lapen et al., 2005; Baird et al., 2008). In contrast, the greater reactivity of the central area could have both stronger (more marked and rapidly perceptible) ecological and biogeochemical consequences under climate change (e.g., Jassey et al., 2013; 2017). From a management point of view, this justifies the use of the temporal hydro-statistical modeling proposed here to assess current and future peatland hydrological status.

**b. Modeling temporal variability of WTD from P and PET: inferring vertical heterogeneity**

The implementation of a statistical model through multiple linear relationships between inputs (P, PET) and WTD was performed for TV11, TV12, TV13, TV14 between the 01/11/2015 and the 31/03/2017 for calibration (i.e. from 3 months after the restoration) and between the 01/04/2017 to the 31/08/2018 for validation. The results of this latter are reported in Figure S3 (supplementary material), and reveal that this may provide consistent trends for TV11, TV12 and TV13 ( $r^2 = 0.25, 0.38, 0.30$  and  $NSE = 0.25, 0.28, 0.26$  respectively). Nevertheless, these indicators remain significantly lower than for the central piezometers, discussed below. This is in accordance with the weaker WTD/P and WTD/PET correlations at the daily scale, implying that the hydrological behavior of the upstream part of the ecosystem responds to complex, and likely delayed, patterns, and suggests that both local peat conductivity and hydraulic connectivity with the surrounding forested peatland and with karst/moraine should be further investigated. For the TV14, the modelling approach is even weaker ( $r^2 = 0.00, NSE = -1.32$ ), in accordance with the observed weak WTD/P and WTD/PET correlations at the daily scale, likely related to its close vicinity with the restored ditch done of imported peat (cf paragraph 4.a).



In contrast, for the central piezometers, (*e.g.*, SoDry), the calibration over 9 hydrological years (3652 daily data) provides a significant matching with observed WTD:  $p\text{-value} < 2.2e-16$ ;  $r^2 = 0,72$  and  $NSE = 0,72$  (Figure 5A,B). This suggests that our approach forms a valuable tool to evaluate hydrological variability and long-term changes for the central area of the active peatland. A good matching is usually observed in spite of differences of up to 4 cm for short and exceptionally dry periods, *e.g.*, in 2011 with WTDs below -19 cm (Figure 5A). For comparison, WTD varies most of the time between -10 and -17 cm. (See Figure S1 in supplementary material).

Model validation for the July 2018-June 2019 period confirms that the linear regression successfully estimates daily variability of the WTD ( $r^2 = 0.86$ ,  $NSE = 0.81$ : Figure 5C). The greatest depths tend to concentrate the largest estimation errors, as observed *e.g.*, for Autumn 2018. This period featured very low precipitation amounts following an extremely dry summer, leading to a historical drought over the region (Le Barbu et al., 2019). A comparable drought was not observed since 1906 and therefore constitutes an extreme event at the scale of our observation period.

This temporary gap for extreme situations suggests that the linear model predicts the greatest depths (extremely low WTD beneath -19 cm) with lower accuracy, as it has been detected through error variance heteroscedasticity for the calibration process (Figure 5B, Breusch-Pagan test  $p < 1.10^{-9}$ ). This could either result from mathematical, hydrophysical (peat hydraulic properties) or ecological reasons that make the ecosystem deviating from a linear behavior under certain hydrological conditions. From a mathematical/statistical point of view, a model better simulates the range of WTDs that frequently occurs, and are therefore better constrained, throughout the calibration period. For comparison purposes, Chen et al. (2002) modelled the WTD of a Canadian aquifer based on a  $r^2$  of 0.60 and  $p\text{-value} < 0.05$  with a set of monthly data over 63 years (756 observed WTD). In a karstic system, Florillo et al. (2010)

showed a one-year  $r^2$  of 0.75. Their results are comparable to ours. Other "black box" approaches such as artificial neural networks (e.g. Multi-Layer Perception Network and long short-term memory models) may present slightly better results (Huang et al., 2019) or can be more efficient for extreme events than reservoir models (Kong A Siou et al 2014). However, altogether our approach yields an overall good projection with a simple and robust method.

The hydrodynamic complexity is higher for peatlands compared to rock aquifers, because the relationships between environmental variables such as evapotranspiration and WTD are more complex and more dynamic (Reeve et al., 2000; Cobat et al., 2004). According to its degree of hydration, peat matrix sees its volume changing, which buffers WTD changes. Additionally, decreasing hydration will also alter the peat pore space and the hydraulic conductivity of peat favoring water retention especially during droughts (Kennedy and Price, 2004). This will in turn affect volume water content, that, combined with pore water pressure (and atmospheric vapor pressure at the air-water interface) in the unsaturated peat will govern capillary rise and impact transpiration rates (Thompson and Waddington, 2008). Ingram (1978), and Morris et al. (2011), stated that statistical patterns may reveal recurrent hydroecological conditions in peatlands. In particular, the frequency distribution of the multi-year water-table average position may allow defining the boundary between the acrotelm (greater K) and catotelm (lower K) corresponding to the absolute largest WTD (Morris et al., 2011). Several authors assess which magnitude or return period of drought should be used to determine the acrotelm–catotelm boundary, and proposed to define this boundary from the annual or five-year drought water table (Ivanov, 1981; Wieder and Vitt, 2006). The weaker matching between observed and simulated WTD through a simple linear method would be consistent with such a limit between a superficial hydrologically active, and a deeper layer with different reactivity to meteorological pulses. It is usually observed that K tends to decrease with depth from the acrotelm to the catotelm (e.g., Bertrand et al., 2012, and

references therein), as they are closely related to the degree of humification of the peat. In the case of the Frasné peatland central area, this functional limit is therefore revealed to occur at -19 cm. Similarly, Jassey et al. (2017) found a hydrological threshold at -24 cm in a peatland in Poland. When WTD was under this limit, the ecosystem respiration was revealed to significantly increase, highlighting the interest in modelling future WTD.

### **c. Projections of the future WTD evolution according to RCP scenarios: Heterogeneity of future hydrological behavior and potential ecohydrological consequences**

Since our model is able to explain 85 % of the WTD variability under current climate conditions, its implementation with daily T and P under RCP 4.5 and RCP8.5 derived from the bias-corrected Euro-CORDEX simulations (paragraph 2.d.) allows calculating future WTD trends for the central area of the peatland (Figure 6).

Comparing the observed 2009-2019 WTD average (-14.6 cm) with the modeled values reveals that annual WTD means could significantly change in the future, and that this change could evolve at various rates depending on the RCP (Figure 6). Two main phases may be delineated from these projections: (1) a rather constant mean WTD until the mid 21<sup>st</sup> century, regardless the considered RCP (2) from the 2050s-2060s, a clear differentiation appears between the RCPs, in line with their divergent radiative pathway during the second half of the century. RCP4.5 features a moderately lower mean WTD (-14.8 cm in average) by 2100, while RCP 8.5 characterizes a stronger WTD drop to -15.6 cm (average over the 2090-2100 period). Under both scenarios, long-term changes are superimposed to natural climate variability, chaotic in nature, which is both smoother and weaker in the climate ensemble mean than in the real world because they are not phased from one model to another. Consistently, various studies show that general climatic trends are mostly model dependent rather than RCP dependent for the first half of the 21<sup>st</sup> century. Conversely, after 2050,

differences between RCP become predominant upon model uncertainties (Collins et al., 2014).

In the perspective to delineate future climate change impacts, Moore (2002) suggested the WTD increase induced by rising temperatures and PET could be locally offset by precipitation rise during some period of the year as it was investigated by various authors (*e.g.*, Manabe and Wetherald 1987, Mitchell, 1989, Pachauri et al., 2015). Consistently, much stronger and contrasted seasonal evolutions can be identified over the area and were concealed in the above analyses performed at the annual scale (Figure 7). In particular, while winter WTD remains roughly stable, probably because T increase leading to enhanced evapotranspiration is compensated by more abundant rainfall, transitional seasons of springs and autumns are expected to feature WTD decreases, especially under the RCP8.5 after 2050. This is even more marked for the summer season, which experiences by far the largest changes in magnitude. Another aspect of future climate changes is that summers and autumns display more variable behaviors at the inter-annual scale. These observations are in agreement with regional projections over hydrological systems (Brulebois et al., 2015b).

Projected precipitation amounts over the century are next used to assess current and future drought frequency in the ecosystem. Frequency of occurrence of lower WTD than a given threshold ( $-5$  cm against annual mean) and the persistence of this state during at least 5 consecutive days were calculated (Figure 8). These indicators, integrating the long-term change of average WTD (i.e. mean WTD in 2050 is different of mean WTD in 2100) can be considered as a proxy of the potential seasonal hydric stress. If drought occurs, WTD increases and capillary supply may be exceeded by evaporation at the surface. Hence, the near-surface water content of the peat may dramatically decrease, concurrently with the capillary water content. This could lead to major growth reduction and consequently decrease

in carbon fixation (Gerdol et al., 1996; McNeil and Waddington, 2003; Schipperges and Rydin, 1998; Jassey et al., 2013).

Droughts as defined here are expected to significantly increase in frequency from May to November in comparison to the observed period (2008-2019), under any RCP. For RCP4.5, except in June and October for which a decrease in drought frequency is found, significant increase prevails in July from 2040-2070. They are next stabilized in July, August, September until 2100. RCP8.5 implies a similar drought frequency for the 2010-2040 period (Figure 3). In contrast, 2070-2100 should present much stronger drought frequency, especially in May (frequency=0,1), June (f=0,5), July (f=0,98), September (f=0,8) and October (f=0,3).

Such changes in the drought frequency, especially during the end of spring and summer, could have a range of ecological and biogeochemical impacts over the ecosystem. From an ecological point of view, greater WTD were identified to negatively impact both total production of bryophytes and the diversity of the *Sphagnum* genus because of the competitiveness of vascular plants in less water saturated soils (Weltzin et al., 2001; Buttler et al., 2015). Over several years, colonization by shrubs and trees may potentially trigger complex feedbacks on the WTD. For instance, (Limpens et al., 2014) found in a mesocosm experiment, that as bogs become colonized by trees, the ecosystem water loss changes with time and impact the WTD in complex patterns. In particular, although a drying effect may be observed during first stage of colonization (low tree density), then this effect is increasingly offset by shading effects during the later phases of tree colonization. The proposed modelling approach hardly directly evaluates such non-linear processes that remain to be mechanistically implemented to further refine water balance over peatlands. In addition, microbial community diversity are known to shrink in case of greater WTD (e.g., (Urbanová and Bárta, 2014), especially in the layer featuring the common hydrodynamic part of the peatland, i.e. the acrotelm. Since equilibrium and communication between plant communities are driven by

microorganism-plant interaction, modifications of the medium can cause rapid changes in the composition of the bryophytic diversity (Ruhí et al., 2014).

These changes should therefore alter the ability of the peatland to store atmospheric carbon as peat is dominated by residues of *Sphagnum* mosses mainly composed of recalcitrant organochemical compounds such as polyphenols (Delarue, 2011). Among other parameters (e.g., acidic conditions and low soil temperature), waterlogging was recognized to limit the activity of phenoloxidase (Jassey et al., 2011 and references therein), and consequently, favor peat accumulation and carbon sequestration. In this context, the extent to which the expected stronger summer droughts and shallower winter WTD could in fact these processes still needs to be clarified.

In this perspective, comparison between phenol concentrations in tissues measured in 2010 (after Jassey et al., 2011) and expected drought frequencies (Figure 8) shows that, during the growth period in spring and summer phenol concentrations are the lowest during July and August. This probably denotes the effect of lower WTD combined with superficial desiccation of peat during the maximum insolation period (Dorrepaal et al., 2004; Aerts, 2006; Jassey et al., 2011), favoring phenoloxidase production by fungal communities. The projected greater drought frequency for spring and summer in the different RCPs could imply longer duration of such processes, favoring in turn, a larger release of CO<sub>2</sub>, as it was recently detected at Frasne during the historical drought of the summer 2018 (Lhosmot et al., 2019).

## 5. Conclusions

This work aims at illustrating the relevance of linear modelling from simple meteorological variables for assessing the impact of climate change on WTD in peatland ecosystems. The results yield a spatial picture of WTD reactivity over the Frasne peatland, to be related to gradients in peat maturity and fiber content. This horizontal variability of the

peatland hydrological behavior highlights its structural heterogeneity. This is also true along the vertical axis, structured by different pedo-hydrological compartments acrotelm, catotelm.

For peatlands, the interest of such analyses of long-term hydrological variability, under changing meteorological and climate conditions, is twofold. Firstly, the hydrodynamic limit between acrotelm and catotelm can be identified. Secondly, this approach can be used to link WTD to input parameters, such as P and estimated PET from T. The significant fit between the multiple linear regression and observations at the center of the system, can next be used to propose ecohydrological scenarios of the peatland long-term evolutions under climate change. In this regard, the hydrodynamic limit at  $-10$  cm identified for the central piezometer, and the difficulty to tightly model WTD under this threshold, remain a limitation intrinsically linked to the linear nature of the model. This justifies why the model was then used to focus on seasonal and climatic trends but that is still limited to date for finer time resolutions. This limitation is also related to the use of several daily meteorological simulations that do not synchronize the occurrence of extreme situations (e.g. droughts). Some efforts, *e.g.*, by proposing a sub-model applying for extremely dry and prolonged conditions could be further planned to fix this specificity, though that effort for longer monitoring is necessary to provide sufficient data for a specific sub-model fitting greatest WTD. This possible limitation should also be highlighted for areas presenting a stronger seasonality in precipitations, as daily precipitation impacts could be more difficult to delineate from the proposed cross-correlation analysis. In this case, the approach formerly proposed by Chen et al. (2002) should be tested.

Despite these constraints for local or temporary situations, our results suggest that on-going climate changes impact both annual and seasonal conditions. While annual WTD remains stable until the first half of the 21<sup>st</sup> century under the two tested RCPs, a clearly distinct behavior is obtained during the second half of the century, showing much stronger

WTD decline for the RCP8.5. At the seasonal scale, this distinct trajectory should have strong consequences in terms of carbon balance, especially by increasing summertime carbon production, under more intense, more persistent and more frequent drought conditions.

Based on these observations, stakeholders and peatland managers should consider that investments in relatively simple monitoring equipment could constitute, when implemented over the long-term, a very efficient way to quantify these variabilities, to identify their ecohydrological causes, and to forecast the consequences for future climate scenarios. This also underlines the importance of structuring Critical Zone monitoring networks (*e.g.*, Anderson et al., 2004; Gaillardet et al., 2018) as a powerful tool to help scientific and stakeholder communities to work together in order to optimize the management of these highly sensitive ecosystems during climate change.

## Acknowledgements

The authors warmly thank the managers of the Regional Natural reserve of Frasné-Bouvenans for allowing access to the site. This study was supported by the SNO Tourbières (<https://www.sno-tourbieres.cnrs.fr/>) and the French network of critical zone observatories (OZCAR) Network (<https://www.ozcar-ri.org/fr/ozcar-observatoires-de-la-zone-critique-applications-et-recherche/>). The SNO Tourbières observing system <https://www.sno-tourbieres.cnrs.fr/> was set up thanks to an incentive funding of the French Ministry of Research that allowed pooling together various pre-existing small scale observing setups. The continuity and long term perenity of the measurements are made possible by an undisrupted and continuous CNRS-INSU funding since 2008. Regionalized climate projections were downloaded from the Drias-Climat platform (<http://www.drias-climat.fr/>). A. Ponçot benefited a financial support from the BIOGEO theme of the Laboratory Chrono-Environnement (UMR UFC CNRS 6249). Finally, the authors warmly thank Pr. François Gillet for its help in writing R scripts and the two anonymous reviewers that provided detailed remarks and suggestions allowing a significant improvement of the manuscript.



## References

- Aerts, R., 2006. The freezer defrosting: global warming and litter decomposition rates in cold biomes: Global warming and litter decomposition. *Journal of Ecology* 94, 713–724. <https://doi.org/10.1111/j.1365-2745.2006.01142.x>
- Anderson, S.P., Blum, J., Brantley, S.L., Chadwick, O., Chorover, J., Derry, L.A., Drever, J.I., Hering, J.G., Kirchner, J.W., Kump, L.R., Richter, D., White, A.E., 2004. Proposed initiative would study Earth's weathering engine. *Eos Trans. AGU* 85, 265. <https://doi.org/10.1029/2004EO280001>
- Augustin, J., Merbach, W., Rogasik, J., 1998. Factors influencing nitrous oxide and methane emissions from minerotrophic fens in northeast Germany. *Biology and Fertility of Soils* 28, 1–4. <https://doi.org/10.1007/s003740050455>
- Aussenac, G., Boulangeat, C., 1980. Interception des précipitations et évapotranspiration réelle dans des peuplements de feuillu (*Fagus sylvatica* L.) et de résineux (*Pseudotsuga menziesii* (Mirb) Franco). *Ann. For. Sci.* 37, 91–107. <https://doi.org/10.1051/forest:19800201>
- Baird, A.J., Eades, P.A., Surridge, R.W.J., 2008. The hydraulic structure of a raised bog and its implications for ecohydrological modelling of bog development. *Ecohydrol.* 1, 289–298. <https://doi.org/10.1002/hco.33>
- Bernard-Jannin, L., Binet, S., Gogo, S., Leroy, F., Défarge, C., Jozja, N., Zocatelli, R., Perdereau, L., Laggoun-Défarge, F., 2018. Hydrological control of dissolved organic carbon dynamics in a rehabilitated Sphagnum-dominated peatland: a water-table based modelling approach. *Hydrol. Earth Syst. Sci.* 22, 4907–4920. <https://doi.org/10.5194/hess-22-4907-2018>
- Bertrand, G., Goldscheider, N., Gobat, J.-M., Hunkeler, D., 2012. Review: From multi-scale conceptualization to a classification system for inland groundwater-dependent ecosystems. *Hydrogeol J* 20, 5–25. <https://doi.org/10.1007/s10040-011-0791-5>

- Bierkens, M.F.P., Knotters, M., Hoogland, T., 2001. Space-time modeling of water table depth using a regionalized time series model and the Kalman Filter. *Water Resour. Res.* 37, 1277–1290. <https://doi.org/10.1029/2000WR900353>
- Bongaarts, J., 2019. IPBES, 2019. Summary for policymakers of the global assessment report on biodiversity and ecosystem services of the Intergovernmental Science-Policy Platform on Biodiversity and Ecosystem Services. *Population and Development Review* 45, 680–681. <https://doi.org/10.1111/padr.12283>
- Bouchet, R. J., 1963. Evapotranspiration réelle et potentielle, signification climatique. *IAHS Publ*, 62, 134-142.
- Bourgault, M.-A., Larocque, M., Garneau, M., 2019. How do hydrogeological setting and meteorological conditions influence water table depth and fluctuations in ombrotrophic peatlands? *Journal of Hydrology X* 4, 100032. <https://doi.org/10.1016/j.hydroa.2019.100032>
- Box, G.E.P., Jenkins, G.M. and Reinsel, G.C., 1994. *Time Series Analysis; Forecasting and Control*. 3rd Edition, Prentice Hall, Englewood Cliff, New Jersey.
- Briot, M., 2004. Restauration des capacités biogènes des tourbières: Etude hydrogéologique, hydrologique, et pédologique d'une zone sous influence d'un drain dans la Réserve Naturelle de Frasne (Doubs, France) (Rapport de stage). SMMMAHD.
- Brulebois, E., Castel, T., Richard, Y., Chateau-Smith, C., Amiotte-Suchet, P., 2015a. Hydrological response to an abrupt shift in surface air temperature over France in 1987/88. *Journal of Hydrology* 531, 892–901. <https://doi.org/10.1016/j.jhydrol.2015.10.026>
- Brulebois, E., Ubertosi, M., Bachmann, J., Rossi, A., Castel, T., Richard, Y., Sauvage, S., Sanchez Perez, J.-M., and Amiotte-Suchet, P. 2015b. Sensitivity of water quality of three contrasted north-eastern French watersheds to climate change (2006-2100) using SWAT model. International SWAT conference. (Pula, Sardinia, Italy).
- Buttler, A., Robroek, B.J.M., Laggoun-Défarage, F., Jassey, V.E.J., Pochelon, C., Bernard, G., Delarue, F., Gogo, S., Mariotte, P., Mitchell, E.A.D., Bragazza, L., 2015. Experimental warming

- interacts with soil moisture to discriminate plant responses in an ombrotrophic peatland. *J Veg Sci* 26, 964–974. <https://doi.org/10.1111/jvs.12296>
- Chen, Z., Grasby, S.E., Osadetz, K.G., 2002. Predicting average annual groundwater levels from climatic variables: an empirical model. *Journal of Hydrology* 260, 102–117. [https://doi.org/10.1016/S0022-1694\(01\)00606-0](https://doi.org/10.1016/S0022-1694(01)00606-0)
- Collin L., 2016. Établissement d'un modèle conceptuel du fonctionnement hydro-écologique de la tourbière de Frasne. Master thesis, Univ. Of Franche-Comté, 86 p.
- Collins, M., R. Knutti, J. Arblaster, J.-L. Dufresne, T. Fifefer, P. Friedlingstein, X. Gao, W.J. Gutowski, T. Johns, G. Krinner, M. Shongwe, C. Tebaldi, A.J. Weaver and M. Wehner, 2013: Long-term Climate Change: Projections, Commitments and Irreversibility. In: *Climate Change 2013: The Physical Science Basis. Contribution of Working Group I to the Fifth Assessment Report of the Intergovernmental Panel on Climate Change* [Stocker, T.F., D. Qin, G.-K. Plattner, M. Tignor, S.K. Allen, J. Boschung, A. Nauels, Y. Xia, V. Bex and P.M. Midgley (eds.)]. Cambridge University Press, Cambridge, United Kingdom and New York, NY, USA.
- Delbart, C., Valdes, D., Barbecot, F., Tognelli, A., Richon, P., Couchoux, L., 2014. Temporal variability of karst aquifer response time established by the sliding-windows cross-correlation method. *Journal of Hydrology* 511, 580–588. <https://doi.org/10.1016/j.jhydrol.2014.02.008>
- Dorrepaal, E., Aerts, R., Cornelissen, J.H.C., Callaghan, T.V., van Logtestijn, R.S.P., 2004. Summer warming and increased winter snow cover affect *Sphagnum fuscum* growth, structure and production in a sub-arctic bog. *Global Change Biol* 10, 93–104. <https://doi.org/10.1111/j.1365-2486.2003.00718.x>
- Dryas-Climat, 2019. [www.dryas-climat.fr](http://www.dryas-climat.fr) Accessed the 02 jan 2019
- Eppinga, M.B., de Ruiter, P.C., Wassen, M.J., Rietkerk, M., 2009. Nutrients and Hydrology Indicate the Driving Mechanisms of Peatland Surface Patterning. *The American Naturalist* 173, 803–818. <https://doi.org/10.1086/598487>

Gaillardet, J., Braud, I., Hankard, F., Anquetin, S., Bour, O., Dorfliger, N., de Dreuzy, J.R., Galle, S., Galy, C., Gogo, S., Gourcy, L., Habets, F., Laggoun, F., Longuevergne, L., Le Borgne, T., Naaïm-Bouvet, F., Nord, G., Simonneaux, V., Six, D., Tallec, T., Valentin, C., Abril, G., Allemand, P., Arènes, A., Arfib, B., Arnaud, L., Arnaud, N., Arnaud, P., Audry, S., Comte, V.B., Batiot, C., Battais, A., Bellot, H., Bernard, E., Bertrand, C., Bessière, H., Binet, S., Bodin, J., Bodin, X., Boithias, L., Bouchez, J., Boudevillain, B., Moussa, I.B., Branger, F., Braun, J.J., Brunet, P., Caceres, B., Calmels, D., Cappelaere, B., Celle-Jeanton, H., Chabaux, F., Chalikakis, K., Champollion, C., Copard, Y., Cotel, C., Davy, P., Deline, P., Delrieu, G., Demarty, J., Dessert, C., Dumont, M., Emblanch, C., Ezzaoui, J., Estèves, M., Favier, V., Fauchoux, M., Filizola, N., Flammarion, P., Floury, P., Fovet, O., Fournier, M., Francez, A.J., Gandois, L., Gascuel, C., Gayer, E., Genthon, C., Gerard, M.F., Gilbert, D., Gouttevin, I., Grippa, M., Gruau, G., Jardani, A., Jeanneau, L., Jomès, J.L., Jourde, H., Karbou, F., Labat, D., Lagadeuc, Y., Lajeunesse, E., Lastennet, P., Lavado, W., Lawin, E., Lebel, T., Le Bouteiller, C., Legout, C., Lejeune, Y., Le Moir, E., Le Moigne, N., Lions, J., Lucas, A., Malet, J.P., Marais-Sicre, C., Maréchal, J.C., Marlin, C., Martin, P., Martins, J., Martinez, J.M., Massei, N., Mauclerc, A., Mazzilli, M., Molénat, J., Moreira-Turcq, P., Mougin, E., Morin, S., Ngoupayou, J.N., Panthou, G., Peugeot, C., Picard, G., Pierret, M.C., Porel, G., Probst, A., Probst, J.L., Rabatel, A., Paclot, D., Ravanel, L., Rejiba, F., René, P., Ribolzi, O., Riotte, J., Rivière, A., Robain, H., Ruiz, L., Sanchez-Perez, J.M., Santini, W., Sauvage, S., Schoeneich, P., Seidel, J.L., Sekkar, M., Sengtaheuanghong, O., Silvera, N., Steinmann, M., Soruco, A., Tallec, G., Thibert, E., Lao, D.V., Vincent, C., Viville, D., Wagnon, P., Zitouna, R., 2018. OZCAR: The French Network of Critical Zone Observatories. *Vadose Zone Journal* 17, 180067. <https://doi.org/10.2136/vzj2018.04.0067>

Gauthier, E., Jassey, V.E.J., Mitchell, E.A.D., Lamentowicz, M., Payne, R., Delarue, F., Laggoun-Defarge, F., Gilbert, D., Richard, H., 2019. From Climatic to Anthropogenic Drivers: A Multi-Proxy Reconstruction of Vegetation and Peatland Development in the French Jura Mountains. *Quaternary* 2, 38. <https://doi.org/10.3390/quat2040038>

- Gendry, M. (2018) La réserve utile des sols. Bulletin sol et agronomie des chambres d'agriculture des pays de la Loire, n°4 du 02/05/2018
- Gerdol, R., Bonora, A., Gualandri, R., Pancaldi, S., 1996. CO<sub>2</sub> exchange, photosynthetic pigment composition, and cell ultrastructure of Sphagnum mosses during dehydration and subsequent rehydration. *Can. J. Bot.* 74, 726–734. <https://doi.org/10.1139/b96-091>
- Gobat, J-M., Aragno M., Matthey W. (2004) The living soil. Science, Enfield, NS, Canada
- Goubet, P., 2015. Résultat d'expertise de l'analyse des macrorestes de carottes de tourbe de la tourbière active de Frasne (25, France).
- Grosvernier P., 2014. Fermeture de fossés au Creux au Lard, tourbière du Forbonnet (Commune de Frasne, France). Compte-rendu d'étude du cabinet L'in'ECO, SMMAHD.
- Guillot, P., & Duband, D., 1980. Une méthode de transfert pluie-débit par régression multiple. *Hydrological Forecasting*, 177-186
- Huang X , Gao L., Crosbie RS, Zhang N, Furti, Doble R., 2019. Groundwater Recharge Prediction Using Linear Regression, Multi-Layer Perception Network, and Deep Learning. *Water* 2019, 1879. doi:10.3390/w11091879
- Ingram HAP., 1978. Soil layers in loires: function and terminology. *Journal of Soil Science* 29: 224–227
- Jacob, D., Petersen, J., Egge t, B., Alias, A., Christensen, O.B., Bouwer, L.M., Braun, A., Colette, A., Déqué, M., Georgievski, G., Georgopoulou, E., Gobiet, A., Menut, L., Nikulin, G., Haensler, A., Hempelmann, N., Jones, C., Keuler, K., Kovats, S., Kröner, N., Kotlarski, S., Kriegsmann, A., Martin, E., van Meijgaard, E., Moseley, C., Pfeifer, S., Preuschmann, S., Radermacher, C., Radtke, K., Rechid, D., Rounsevell, M., Samuelsson, P., Somot, S., Soussana, J.-F., Teichmann, C., Valentini, R., Vautard, R., Weber, B., Yiou, P., 2014. EURO-CORDEX: new high-resolution climate change projections for European impact research. *Reg Environ Change* 14, 563–578. <https://doi.org/10.1007/s10113-013-0499-2>

- Jassey, V.E.J., Chiapusio, G., Gilbert, D., Buttler, A., Toussaint, M.-L., Binet, P., 2011. Experimental climate effect on seasonal variability of polyphenol/phenoloxidase interplay along a narrow fen-bog ecological gradient in *Sphagnum fallax*: PHENOL/PHENOLOXIDASE INTERPLAY IN PEATLAND. *Global Change Biology* 17, 2945–2957. <https://doi.org/10.1111/j.1365-2486.2011.02437.x>
- Jassey, V.E., Chiapusio, G., Binet, P., Buttler, A., Laggoun-Défarge, F., Delarue, F., Bernard, N., Mitchell, E.A., Toussaint, M.-L., Francez, A.-J., Gilbert, D., 2013. Above- and belowground linkages in *Sphagnum* peatland: climate warming affects plant-microbial interactions. *Glob Change Biol* 19, 811–823. <https://doi.org/10.1111/gcb.12075>
- Jassey, V.E.J., Reczuga, M.K., Zielińska, M., Słowińska, S., Roelofs, B.J.M., Mariotte, P., Seppey, C.V.W., Lara, E., Barabach, J., Słowiński, M., Dagała, L., Chojnicki, B.H., Lamentowicz, M., Mitchell, E.A.D., Buttler, A., 2018. Tipping point in plant–fungal interactions under severe drought causes abrupt rise in peatland ecosystem respiration. *Glob Change Biol* 24, 972–986. <https://doi.org/10.1111/gcb.14928>
- Jassey, V.E.J., Signarbieux, C., 2019. Effects of climate warming on *Sphagnum* photosynthesis in peatlands depend on peat moisture and species-specific anatomical traits. *Glob Change Biol* 25, 3859–3870. <https://doi.org/10.1111/gcb.14788>
- Jenkins, G. M. and Watt, D. G., 1968. *Spectral Analysis and Its Applications* Holden-Day. San Francisco, 243-238.
- Joosten, H., 2016. Peatlands across the globe, in: Bonn, A., Allott, T., Evans, M., Joosten, H., Stoneman, R. (Eds.), *Peatland Restoration and Ecosystem Services*. Cambridge University Press, Cambridge, pp. 19–43. <https://doi.org/10.1017/CBO9781139177788.003>
- Joosten, H., Clarke, D., 2002. *Wise use of mires and peatlands: background and principles including a framework for decision-making*. International Peat Society ; International Mire Conservation Group, Jyväskylä] : [Greifswald.

- Kang, H., Freeman, C., 2002. The Influence of Hydrochemistry on Methane Emissions from Two Contrasting Northern Wetlands. *Water, Air, and Soil Pollution* 141: 263–272.
- Kennedy, G.W., Price, J.S., 2004. Simulating soil water dynamics in a cutover bog: A SIMULATION MODEL FOR A CUTOVER BOG. *Water Resour. Res.* 40. <https://doi.org/10.1029/2004WR003099>
- Kløve, B., Ala-Aho, P., Bertrand, G., Gurdak, J.J., Kupfersberger, H., Kværner, J., Muotka, T., Mykrä, H., Preda, E., Rossi, P., Uvo, C.B., Velasco, E., Pulido-Velazquez, M., 2014. Climate change impacts on groundwater and dependent ecosystems. *Journal of Hydrology* 518, 250–266. <https://doi.org/10.1016/j.jhydrol.2013.06.037>
- Kong-A-Siou, L., Fleury, P., Johannet, A., Borrell Estupina, V., Pistre, S. and Dörfliger N. Performance and complementarity of two systemic models (reservoir and neural networks) used to simulate spring discharge and piezometry for a karst aquifer. *Journal of Hydrology*, 519(D), 3178-3192, 2014.
- Krasnostein, A.L., Oldham, C.E., 2004. Predicting wetland water storage: *Water Resour. Res.* 40. <https://doi.org/10.1029/2003WR002039>
- Krause, P., Boyle, D.P., Bäse, F., 2005. Comparison of different efficiency criteria for hydrological model assessment. *Adv. Geosci.* 5, 89–97. <https://doi.org/10.5194/adgeo-5-89-2005>
- Laggoun-Défarge, F., 2008. Les tourbières et leur rôle de stockage de carbone face aux changements climatiques. *Zones Humides Infos* 22–24.
- Laggoun-Défarge, F., Gogo, S., Bernard-Jannin, L., Guimbaud, C., Zocatelli, R., Rousseau, J., Binet, S., D'angelo, B., Leroy, F., Jozja, N., Moing, F.L., Défarge, C., 2016. Does hydrological restoration affect greenhouse gases emission and plant dynamics in sphagnum peatlands? *Mires and Peat*, in press 5.
- Lapen, D.R., Price, J.S., Gilbert, R., 2005. Modelling two-dimensional steady-state groundwater flow and flow sensitivity to boundary conditions in blanket peat complexes. *Hydrol. Process.* 19, 371–386. <https://doi.org/10.1002/hyp.1507>

- Lavoie, M., Larouche, A.C., Richard, P.J.H., 2007. Conditions du développement de la tourbière de Farnham, Québec. *GPQ* 49, 305–316. <https://doi.org/10.7202/033044ar>
- Le Barbu E., Philippe M., Cadet Y., 2019. Sécheresse 2018 dans le Haut-Doubs : du jamais vu depuis 1906. Colloque UNESCO-SHF : « Sécheresses 2019, Paris 11-12 et 13 Décembre 2019
- Lhosmot, A., Bertrand, G., Steinmann, M., Jacotot, A., Ponçot, A., Collin, L., Toussaint, M.-L., Gogo, S., Magnon, G., Stefani, V., Loup, C., Jeanton, H., Walter, A.-V., Bichet, V., Gilbert, D., Crini, N., Gandois, L., Denimal, S., Moquet, J.-S., Binet, S., Binet, P., Pinel, S., Winiarski, T., Laggoun-Défarge, F., Graillet, D., Paron, F., Caldirak, H., Levastre, V., 2019. CRITICAL PEAT project : The importance of hydrology for Carbon Reservoir along with atmosphere - peatland interactions. Preliminary results from the Fasné peatland monitoring (Jura Mountains, France). Presented at the 2019 Fall Meeting, AGU, San Francisco, CA, 9-13 Dec.
- Limpens, J., Holmgren, M., Jacobs, C.M.J., Van der Zee, S.E.A.T.M., Karofeld, E., Berendse, F., 2014. How Does Tree Density Affect Water Loss of Peatlands? A Mesocosm Experiment. *PLoS ONE* 9, e91748. <https://doi.org/10.1371/journal.pone.0091748>
- Manabe, S. and R.T. Wetherald, 1987. Large scale changes of soil wetness induced by an increase in atmospheric carbon dioxide. *J Atmos Sci.*, 44, 1211-1235.
- Mangin, A., 1975. Contribution à l'étude hydrodynamique des aquifères karstiques. Thèse de Doctorat d'Etat, Université de Dijon Thesis
- Mangin, A., 1984. Pour une meilleure connaissance des systèmes hydrologiques à partir des analyses corrélatrice et spectrale. *J. Hydrol.* 67 (1-4), 25-43.
- Manneville, O., Vergne, V., Villepoux, O., 2006. Le monde des tourbières et des marais, France, Suisse, Belgique, Luxembourg., Delachaux et Niestlé. ed.
- Martin, C., Didon-Lescot, J.-F., 2007. Influence d'une tourbière de moyenne montagne sur les écoulements: le cas de la tourbière des Sagnes sur le Mont-Lozère. *Etudes de Géographie Physique* 27-41.



- McNeil, P., Waddington, J.M., 2003. Moisture controls on Sphagnum growth and CO<sub>2</sub> exchange on a cutover bog: Sphagnum CO<sub>2</sub> exchange on a cutover bog. *Journal of Applied Ecology* 40, 354–367. <https://doi.org/10.1046/j.1365-2664.2003.00790.x>
- Michelangeli, P.-A., Vrac, M., Loukos, H., 2009. Probabilistic downscaling approaches: Application to wind cumulative distribution functions. *Geophys. Res. Lett.* 36, L11708. <https://doi.org/10.1029/2009GL038401>
- Mitchell, C.P.J., Branfireun, B.A., Kolka, R.K., 2008. Spatial Characteristics of Net Methylmercury Production Hot Spots in Peatlands. *Environ. Sci. Technol.* 42, 1010–1016. <https://doi.org/10.1021/es0704986>
- Mitchell, J.F.B., 1989. The “Greenhouse” effect and climate change. *Rev. Geophys.* 27, 115. <https://doi.org/10.1029/RG027i001p00115>
- Moore, P.D., 2002. The future of cool temperate bogs. *Envir. Conserv.* 29, 3–20. <https://doi.org/10.1017/S0376892901000324>
- Morris, P.J., Waddington, J.M., Benscoter, B.W., Turetsky, M.R., 2011. Conceptual frameworks in peatland ecohydrology: looking beyond the two-layered (acrotelm-catotelm) model. *Ecohydrol.* 4, 1–11. <https://doi.org/10.1002/eco.191>
- Nash, J.E., Sutcliffe, J.V., 1970. River flow forecasting through conceptual models part I — A discussion of principles. *Journal of Hydrology* 10, 282–290. [https://doi.org/10.1016/0022-1694\(70\)90255-6](https://doi.org/10.1016/0022-1694(70)90255-6)
- Okkonen, J., Kløve, B., 2010. A conceptual and statistical approach for the analysis of climate impact on ground water table fluctuation patterns in cold conditions. *Journal of Hydrology* 388, 1–12. <https://doi.org/10.1016/j.jhydrol.2010.02.015>
- Oudin, L., Hervieu, F., Michel, C., Perrin, C., Andréassian, V., Anctil, F., Loumagne, C., 2005. Which potential evapotranspiration input for a lumped rainfall–runoff model? *Journal of Hydrology* 303, 290–306. <https://doi.org/10.1016/j.jhydrol.2004.08.026>

- Pachauri, R.K., Mayer, L., Intergovernmental Panel on Climate Change (Eds.), 2015. Climate change 2014: synthesis report. Intergovernmental Panel on Climate Change, Geneva, Switzerland.
- Piao, S., Ciais, P., Huang, Y., Shen, Z., Peng, S., Li, J., Zhou, L., Liu, H., Ma, Y., Ding, Y., Friedlingstein, P., Liu, C., Tan, K., Yu, Y., Zhang, T., Fang, J., 2010. The impacts of climate change on water resources and agriculture in China. *Nature* 467, 43–51. <https://doi.org/10.1038/nature09364>
- Porteret, J., 2008. Fonctionnement hydrologique des têtes de bassin versant tourbeuses du Nord-Est du Massif Central (phdthesis). Université Jean Monnet - Saint-Etienne.
- Preston, M.D., Smemo, K.A., McLaughlin, J.W., Basiliko, N., 2012. Peatland Microbial Communities and Decomposition Processes in the James Bay Lowlands, Canada. *Front. Microbio.* 3. <https://doi.org/10.3389/fmicb.2012.00070>
- Reeve, A.S., Siegel, D.I., Glaser, P.H., 2000. Simulating vertical flow in large peatlands. *Journal of Hydrology* 227, 207–217. [https://doi.org/10.1016/S0022-1694\(99\)00183-3](https://doi.org/10.1016/S0022-1694(99)00183-3)
- Ruhí, A., Chappuis, E., Escoriza, D., Jorner, M., Sala, J., Boix, D., Gascón, S., Gacia, E., 2014. Environmental filtering determines community patterns in temporary wetlands: a multi-taxon approach. *Hydrobiologia* 725, 25–39. <https://doi.org/10.1007/s10750-013-1514-9>
- Schipperges, B., Rydin, H., 1998. Response of photosynthesis of Sphagnum species from contrasting microhabitats to tissue water content and repeated desiccation. *New Phytol* 140, 677–684. <https://doi.org/10.1046/j.1469-8137.1998.00311.x>
- Thomas, J., 2015. Tourbière du Creux au Lard. Analyses de sol. Technical report, Scop Sagne, 7 p.
- Thompson, D.K., Waddington, J.M., 2008. Sphagnum under pressure: towards an ecohydrological approach to examining Sphagnum productivity. *Ecohydrol.* 1, 299–308. <https://doi.org/10.1002/eco.31>
- Toussaint, M.L., Bertrand G., Lhosmot A., Gilbert D., Binet P., Jacotot A., Laggoun-Défarage F., 2020a. Soil-meteorological dataset collected at Frasne peatland (Jura Mountains, France) (Version 1.0) [Data set]. Zenodo. <http://doi.org/10.5281/zenodo.3763342>

- Toussaint, M.L., Bertrand G., Lhosmot A., Gilbert D., Binet P., Laggoun-Défarage F., 2020b. Water table depth dataset collected at Frasne peatland (192ha, Jura Mountains, France) (Version 1.0) [Data set]. Zenodo. <http://doi.org/10.5281/zenodo.3763766>
- Trenberth, K., 2011. Changes in precipitation with climate change. *Clim. Res.* 47, 123–138. <https://doi.org/10.3354/cr00953>
- Urbanová, Z., Bárta, J., 2014. Microbial community composition and in silico predicted metabolic potential reflect biogeochemical gradients between distinct peatland types. *FEMS Microbiol Ecol* 90, 633–646. <https://doi.org/10.1111/1574-6941.12422>
- Verhoeven, J.T.A., Toth, E., 1995. Decomposition of *Carex* and *Sphagnum* litter in fens: Effect of litter quality and inhibition by living tissue homogenates. *Soil Biology and Biochemistry* 27, 271–275. [https://doi.org/10.1016/0038-0717\(94\)00183-2](https://doi.org/10.1016/0038-0717(94)00183-2)
- Vidal, J.-P., Martin, E., Franchistéguy, L., Baillon, M., Soubeyroux, J.-M., 2010. A 50-year high-resolution atmospheric reanalysis over France with the Safran system. *Int. J. Climatol.* 30, 1627–1644. <https://doi.org/10.1002/joc.2003>
- Viswanathan, M.N., 1983. The Rainfall/Water-Table Level Relationship of an Unconfined Aquifer. *Groundwater* 21, 49–56. <https://doi.org/10.1111/j.1745-6584.1983.tb00704.x>
- Vorosmarty, C.J., 2000. Global Water Resources: Vulnerability from Climate Change and Population Growth. *Science* 289, 284–288. <https://doi.org/10.1126/science.289.5477.284>
- Wastiaux, C., 2008. Les tourbières sont-elles des éponges régularisant l'écoulement? *Bulletin de la Société géographique de Liège* 10.
- Weltzin, J.F., Harth, C., Bridgham, S.D., Pastor, J., Vonderharr, M., 2001. Production and microtopography of bog bryophytes: response to warming and water-table manipulations. *Oecologia* 128, 557–565. <https://doi.org/10.1007/s004420100691>
- Xu, J., Morris, P.J., Liu, J., Holden, J., 2018. Hotspots of peatland-derived potable water use identified by global analysis. *Nat Sustain* 1, 246–253. <https://doi.org/10.1038/s41893-018-0064-6>

## Figure captions

*Figure 1 : A. Localization and geological context of the Frasne peatland. B. pedological context over the area (From Briot, 2004; modified), C: Localization of automatically monitored full screened piezometers.*

*Figure 2 : Conceptual hydrological balance and fluxes of the Frasne peatland.*

*Figure 3: Monthly averages of daily precipitation and monthly temperatures over the period (2009-2019, 2040-2070, 2070-2100) according to RCP 4.5 and 8.5. Calculated from the 8 available climatic models in Dryas-climat (2019).*

*Figure 4: Cross-correlograms and spatial variability of response and memory times for P-WTD (A) and PET-WTD (B) Data used for this approach are from September 2015 to August 2018 for TV11, 12, 13, 14 to avoid any restoration effect on the statistical analysis. Data from July 2009 to June 2019 were used for the SOWet and SODry piezometers given that mean WTD did not change there after the restoration works.*

*Figure 5 A: Calibration of the linear regression model versus observed WTD (July 2009-July 2018); B: Modelled versus observed values of WTD after calibration. C: Model validation from 1<sup>st</sup> of July 2018 - 30<sup>th</sup> of June 2019.*

*Figure 6: 2006-2100 annual projections of P, T, calculated PET and WTD (SODry piezometer in the central area of the Frasne peatland) for RCP4.5 and RCP8.5. Observed annual mean for the 2009-2018 period are indicated*

*Figure 7: Predicted seasonal trends of the Frasne WTD.*

Figure 8 : Frequencies of drought events (defined for  $WTD < WTD_{annual\ mean} - 5$  cm during at least 5 days) over 2010-2040, 2040-2070, 2070-2100 according to the scenarios RCP 4.5 and 8.5

Table 1: EURO-CORDEX ensemble models used in this study

<b>EURO-CORDEX Models</b>	<b>RCP4.5</b>	<b>RCP8.5</b>
ichec-ec-earth_hirham5	X	X
ichec-ec-earth_rca4	X	X
ipsl-ipsl-cm5a-mr_wrf331f	X	
cnrm-cerfacs-cnrm-cm5_rca4	X	X
mohc-hadgem2-es_rca4	X	X
m_pi-esm-lr_cclm4-8-17	X	X
meteir-ecearth_racmo22e	X	

**Declaration of competing interests**

The authors declare that they have no known competing financial interests or personal relationships that could have appeared to influence the work reported in this paper.

The authors declare the following financial interests/personal relationships which may be considered as potential competing interests:

Journal Pre-proof

Credit Author Statement

Guillaume Bertrand : Conceptualization, Methodology, Formal analysis, Investigation, Visualization, Writing original draft , Supervision

Alex Ponçot : Methodology, Formal analysis, Investigation, Visualization, Writing original draft

Benjamin Pohl: Methodology, Formal analysis, Investigation, Visualization, Writing - Review & Editing

Alexandre Lhosmot, Marc Steinmann, Philippe Binet : Visualization, Writing - Review & Editing

Anne Johannet, Sébastien Pinel, Huseyin Caldirak, Guillaume Artigue: Visualization, Methodology, Writing - Review & Editing

Catherine Bertrand, Louis Collin, Marie-Laure Toussaint: Data curation

Geneviève Magnon, Daniel Gilbert, Fatima Laggoun-Deffarge: Funding acquisition, Writing - Review & Editing

Graphical abstract

Highlights

- Ten years of Frasne peatland hydrometeorological was performed
- Cross-correlation highlights spatial hydrological reactivity heterogeneities
- Multiple Linear Modelling was performed under RCP4.5 and RCP8.5 till 2100
- We observe a stable mean WTD under RCP4.5 but a significant increase under RCP8.5;
- Seasonal variability of WTD is expected to increase, especially for RCP8.5;
- Both RCP's imply greater summer WTD, potentially impacting the *Sphagnum* metabolism.

Journal Pre-proof



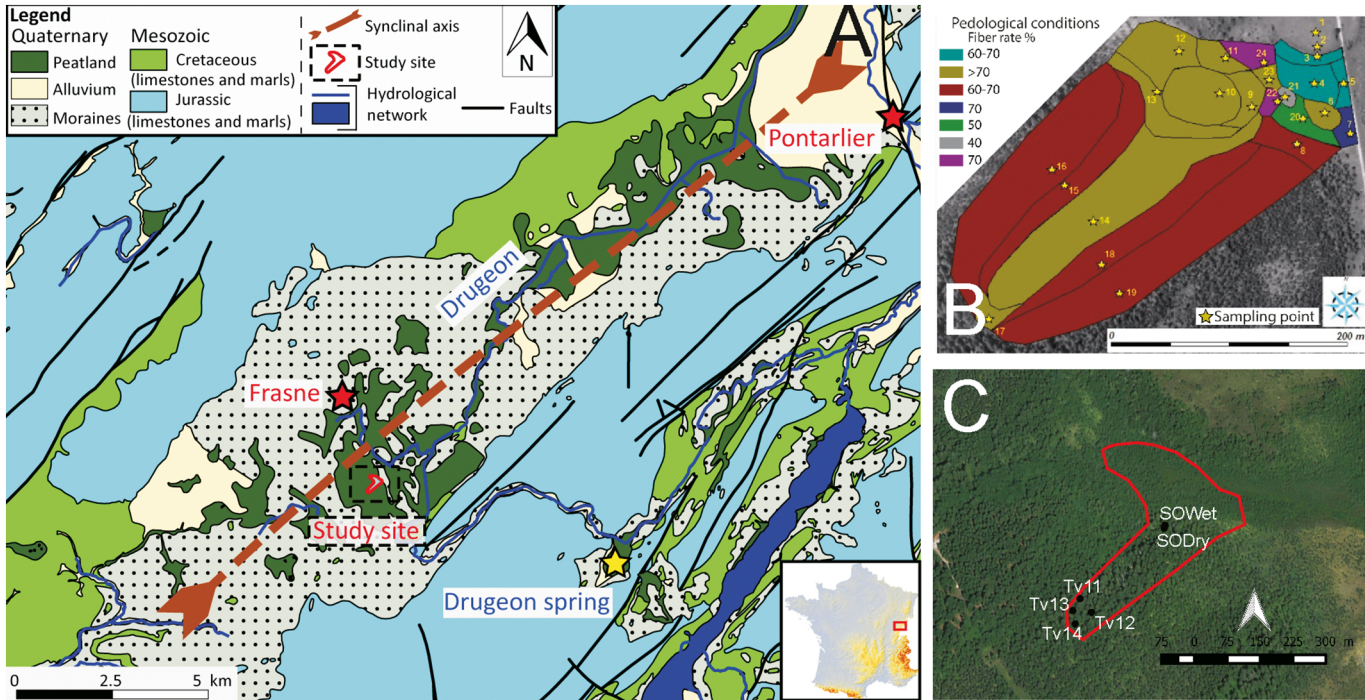
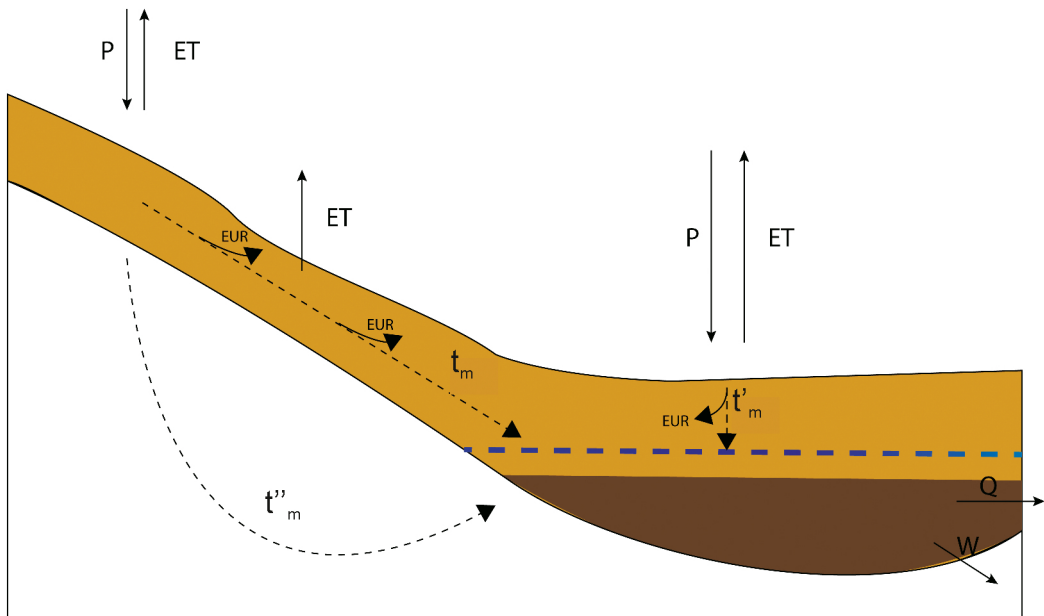


Figure 1



Soil and histosol

Bedrock

Limit of the Saturated area

Catotelm

Water flow (P, ET, Q, W)

Underground path flows

$t_m$  Memory time

P Precipitation

ET Evapotranspiration

EUR Easily Usable water Reserve

Q Surface outflow

W Deep outflow

Figure 2

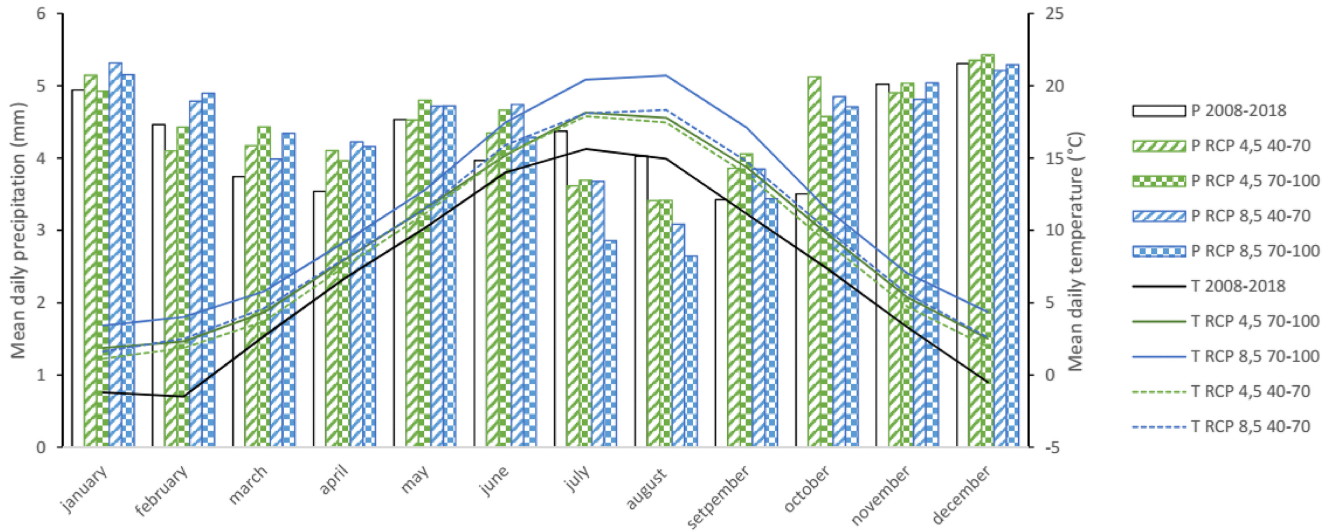


Figure 3

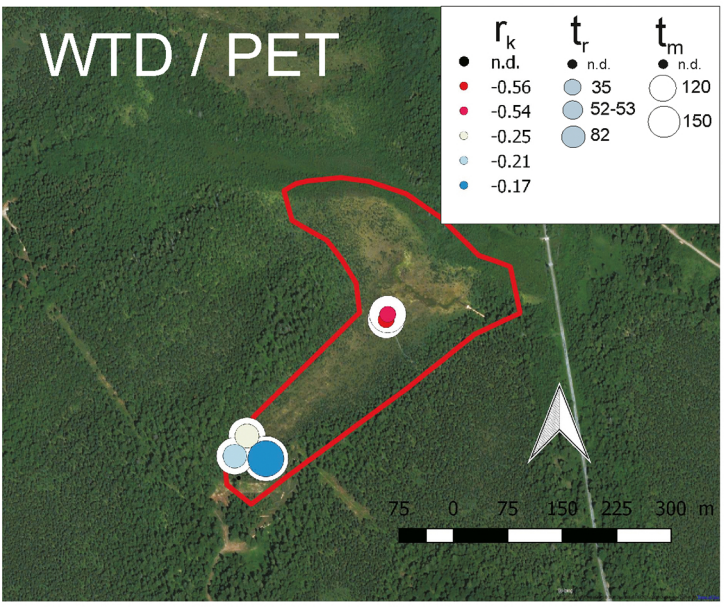
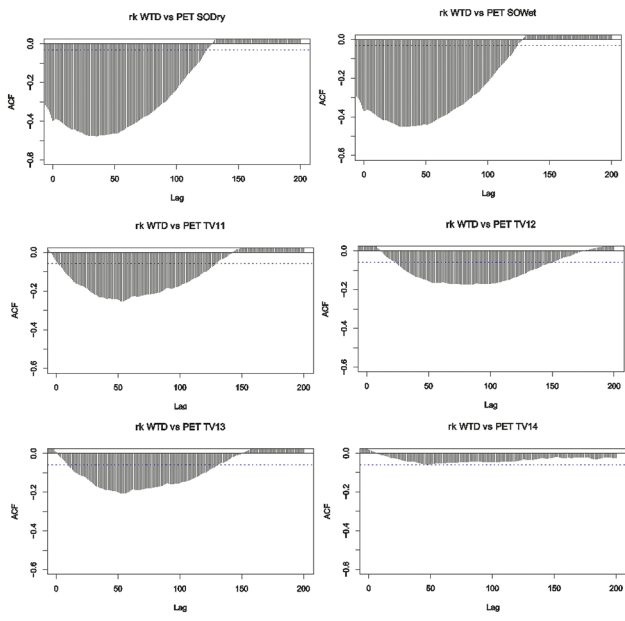
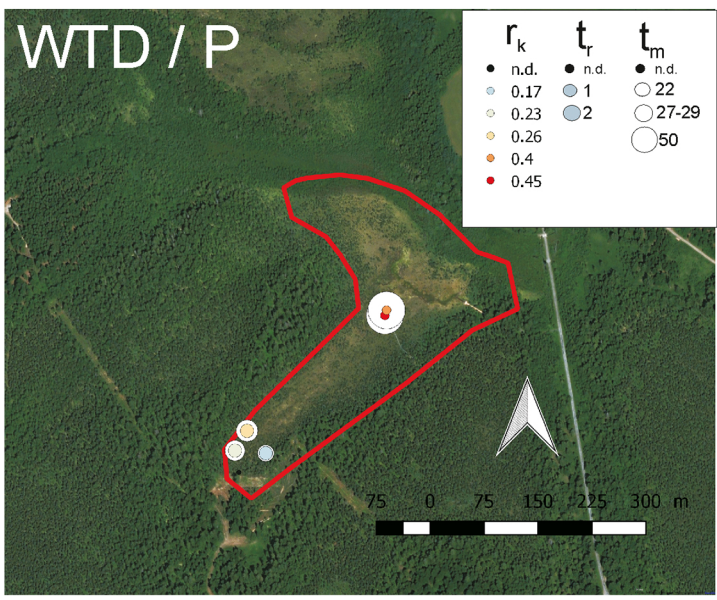
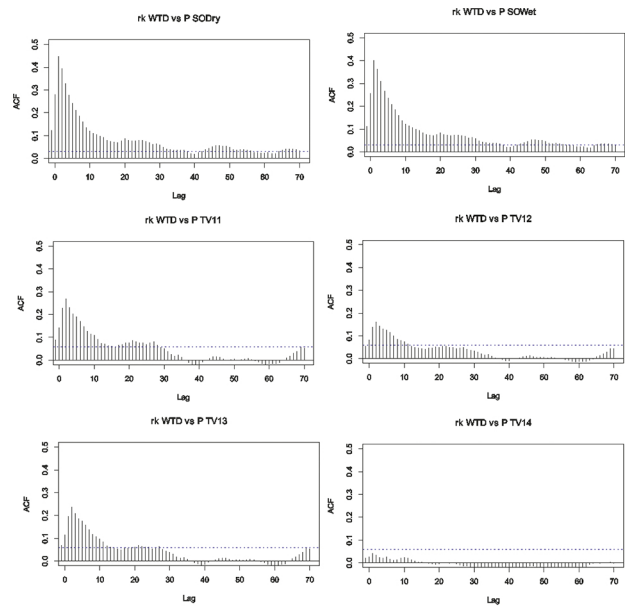


Figure 4

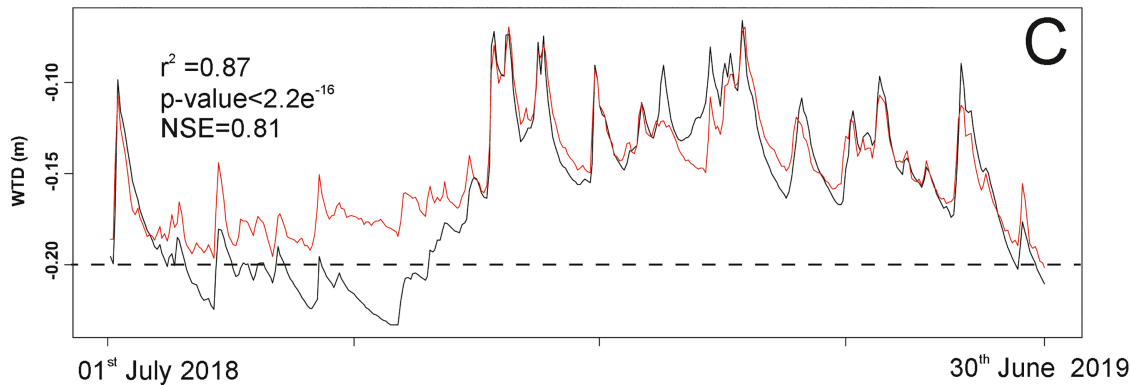
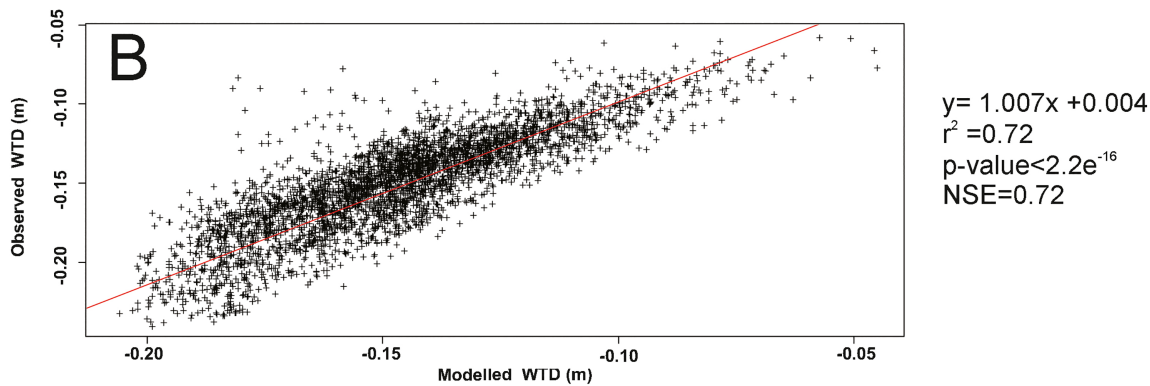
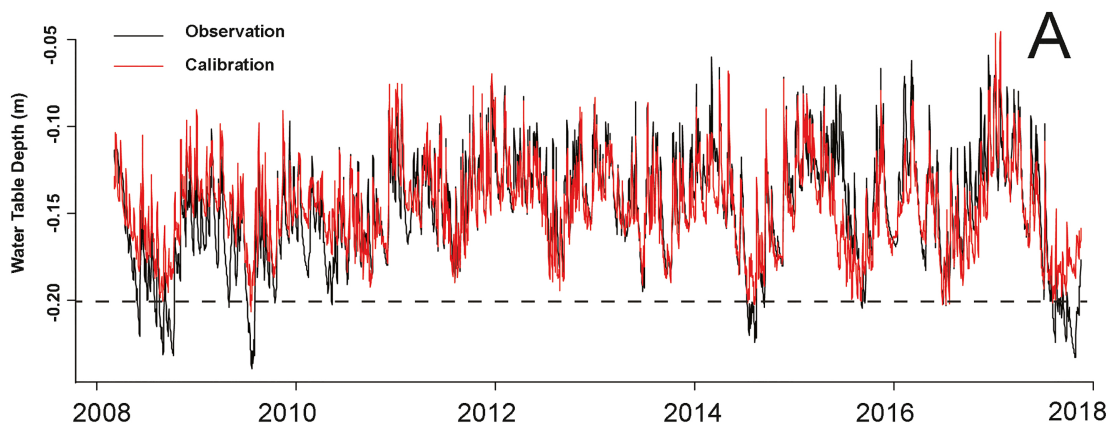


Figure 5

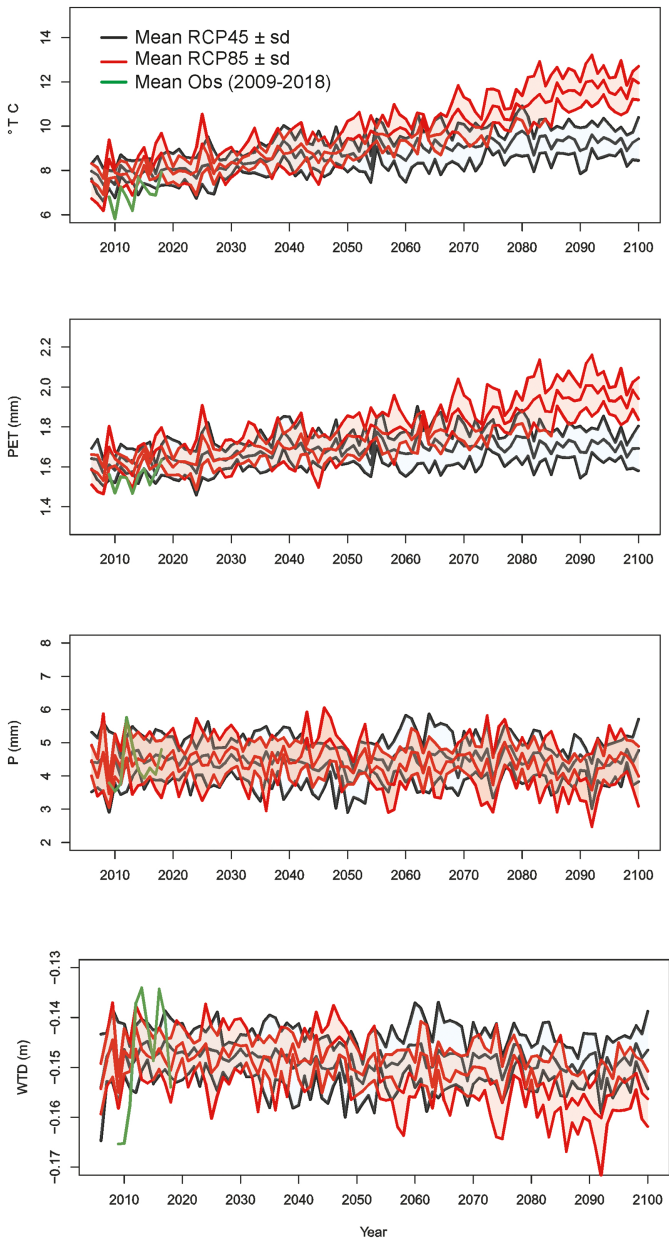


Figure 6

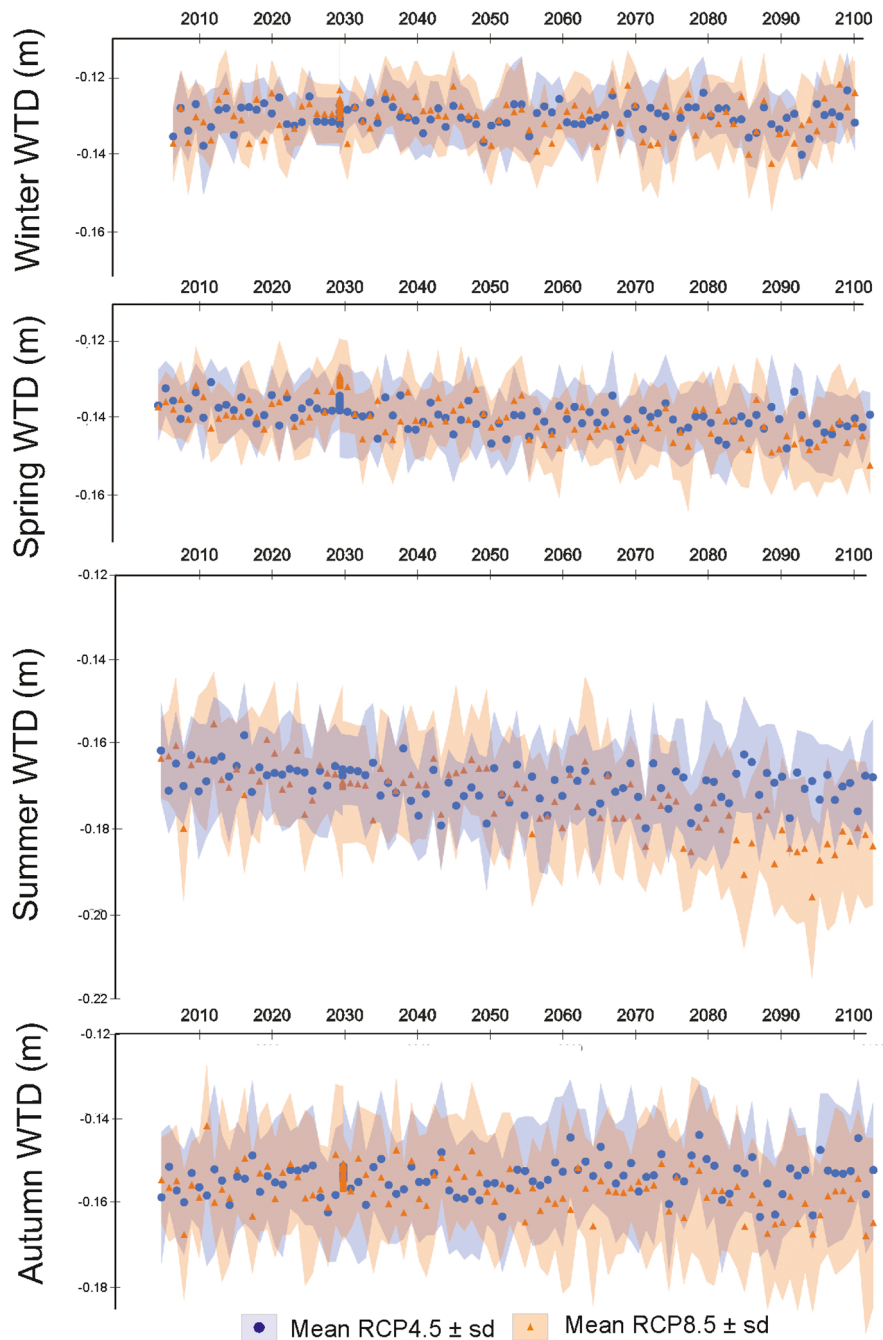


Figure 7

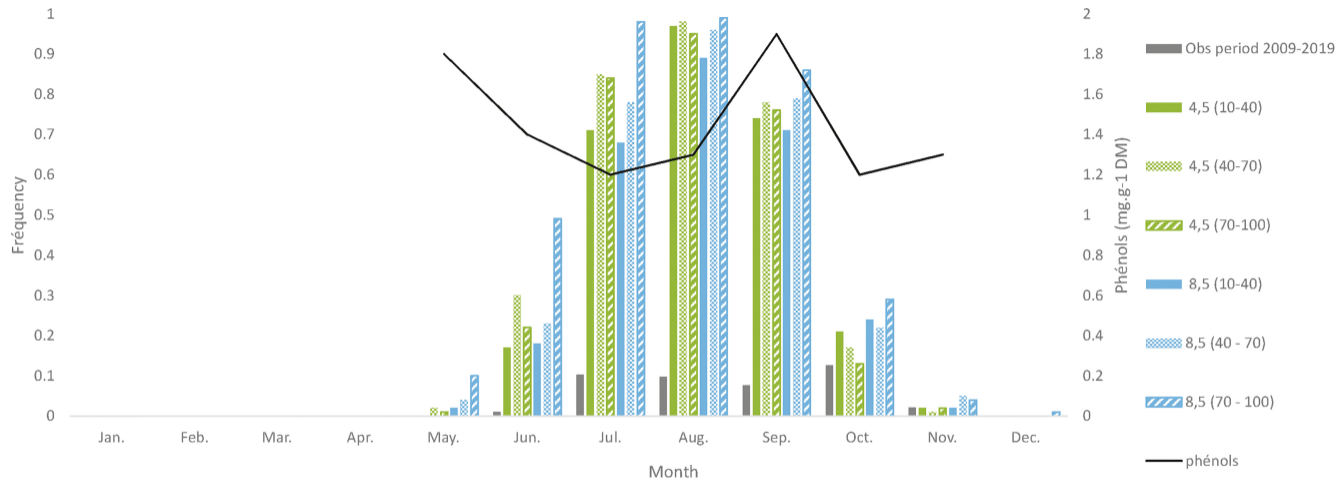


Figure 8